Examensarbete vid Institutionen för geovetenskaper
ISSN 1650-6553 Nr 161

Linguliform Brachiopods from the terminal Cambrian to lower Ordovician Tiñu section, Mexico

Barbro Bornsäter Mellbin

Sammanfattning

Tiñuformationen i Oaxaca, Mexiko är den enda fossilförande enheten från undre paleozoikum mellan den Laurentiska plattformen i nordvästra Mexiko och de Gondwanska lagerföljderna i Sydamerika. Det har nyligen visats att Tiñusektionen är en koncentrerad passiv kantlagerföljd med Gondwanakaraktär. Formationen delas upp i två delar; Yudachica från översta kambrium, som vilar okonformt på mellanproterozoisk grund, och Río Salinas från undre ordovicium (tremadoc). Formationen har tidigare studerats med avseende på dess avsättningsmiljöer och det fossila innehållet av trilobiter och konodonter vilka båda ger utmärkt biostratigrafisk kontroll över formationen.
Ungefär 1000 exemplar av Linguliforma brachiopoder från tolv kalkstenslager från Tiñuformationen har studerats. Detaljerade undersökningar om taxonomi och stratigrafisk distribution av taxa har utförts. Faunan omfattar nio acrotretida taxa och en ny siphonotretid art och ett fåtal lingulida fragment. De acrotretida och det siphonotretida taxa har beskrivits grundligt och klassificerats till släkte.

Nyckelord: Linguliforma, Brachiopoder, Acrotretida, Siphonotretida, Tiñu formationen, Kambrium, Ordovicium

Linguliform Brachiopods from the terminal Cambrian to lower Ordovician Tiñu section, Mexico

Barbro Bornsäter Mellbin

Abstract
The Tiñu Formation of Oaxaca State (Mexico) is the only fossiliferous lower Palaeozoic unit between the Laurentian platform in northwest Mexico and the Gondwanan successions in Andean South America. It has recently been shown that the Tiñu section is a condensed passive margin succession with Gondwanan character. The formation is divided into two members, namely, the uppermost Cambrian Yudachica Member, which rests nonconformably on a middle Proterozoic basement, and the Lower Ordovician (Tremadoc) Río Salinas Member. The formation has been studied with respect to its depositional environments and its fossil content of trilobites and conodonts, both providing excellent biostratigraphical control for the formation.
About 1000 specimens of Linguliform brachiopods of twelve limestone horizons of the Tiñu Formation have been studied. Detailed investigations on taxonomy and stratigraphic distribution of the taxa have been made. The fauna comprises nine acrotretid taxa, a new siphonotretid species and a few linguloid fragments. The acrotretid and siphonotretid taxa have been thoroughly describes and classified to genus.

Keywords: Linguliform, Brachiopods, Acrotretid, Siphonotretid, Tiñu Formation, Cambrian, Ordovician

Introduction

This study deals with the previously undescribed linguliform brachiopod fauna of the Tiñu Formation of Oaxaca State, Mexico. The Tiñu Formation is the only fossiliferous lower Palaeozoic unit between the Laurentian platform in northwest Mexico and the Gondwanan successions in Andean South America and is therefore of great interest, as it can provide information on the area's historical geology. The brachiopod fauna has been described and classified, and an assessment of the changes in brachiopod associations across the Cambrian-Ordovician boundary has been made. This study also presents an excellent basis for continued studies of this brachiopod fauna and its relation to the described environmental changes occurring throughout the formation. It will hopefully also be used for correlation with either Laurentian or west Gondwanan brachiopod faunas in future studies.

Geological setting

As recently as the mid-1960s the fossiliferous Palaeozoic sedimentary rocks were first discovered in Oaxaca State, Mexico by Jerjes Pantoja-Alor (Pantoja-Alor 1965). Prior to this, the following stratigraphic succession had been generally accepted for the area: basal metamorphic rocks of Precambrian or possibly Palaeozoic age (Oaxacan complex), followed by sedimentary deposits of Mesozoic age which are in turn overlain by Cenozoic sedimentary and volcanic rocks (Landing et al. 2006). Pantoja-Alor and Robison (1967) showed that the Palaeozoic sedimentary rocks discovered by Pantoja-Alor (1965) occur as two outliers in the Nochixtlán region that unconformably overlies the Oaxacan complex. The Oaxacan complex was dated to 1 Ga before present by analyses of the pegmatite dikes and, therefore, Precambrian rather than Palaeozoic in age (Pantoja-Alor and Robison 1967). The two Palaeozoic outliers can be found in the Tiñu/Rio Salinas area and in the Barranco de

Santiago Ixtaltepec in central Oaxaca State. They consist of several units of different ages. In both of the outliers, sediments of the upper Cambrian-lowest Ordovician Tiñu Formation rest upon the Precambrian gneiss, which are in the Tiñu outlier directly overlain by Cretaceous limestones and Tertiary red beds (Centeno-Garcia and Keppie 1999; Landing et al. 2006; Pantoja-Alor and Robison 1967; Robison and Pantoja-Alor 1968). The Santiago Ixtaltepec outlier has a different stratigraphy. Here, the Tiñu Formation is overlain by the Early Carboniferous Santiago Formation, which consists of calcareous sandstones, conglomerates, marine limestones, calcareous siltstones and shales. On top of this rest shales, silt-, sand- and limestones of the Late Carboniferous Ixtaltepec Formation (Pantoja-Alor 1970 *fide* Centeno-Garcia and Keppie 1999 and Landing et al. 2007). The contacts between these formations (Tiñu, Santiago and Ixtaltepec) were re-investigated by Centeno-Garcia and Keppie (1999), who showed that both contacts are tectonic rather than unconformities. Over the Ixtaltepec formation lies, unconformably, the Yododeñe Formation, made up of conglomerates, sandstones, siltstones and shales. This formation was interpreted by Pantoja-Alor (1993 *fide* Centeno-Garcia and Keppie 1999) as middle Carboniferous to middle Permian in age, but clasts of limestones in the formation turned out to be of lower Permian origin which suggest that the formation might be younger (Centeno-Garcia and Keppie 1999). On top of the outlier lie Cretaceous marine limestones and Tertiary red beds, which also are found at the Tiñu outlier (Centeno-Garcia and Keppie 1999).

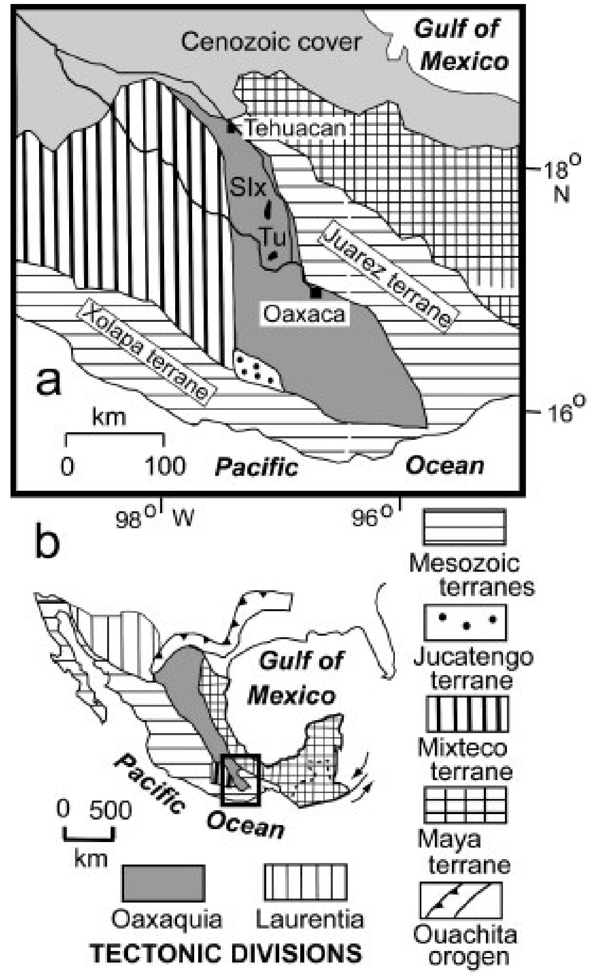

Fig. 1 Generalized locality maps.
(a) Upper Cambrian and lowest Ordovician outliers of the Tiñu Formation (the small black areas) at the Tiñu (Tu) and Barranco de Santiago Ixtaltepec (SIx) inliers on the Oaxaca Complex, Oaxaca State.
(b) Main tectonic subdivisions of Mexico.
(Map from Landing et al. 2007).

Tiñu Formation

The Tiñu Formation in Oaxaca State provides the only record of fossiliferous lower Palaeozoic rocks south of the Laurentian successions in Texas and northern Mexico and north of the Gondwanan sequences in Andean Columbia. It nonconformably overlies the middle Proterozoic metamorphics and intrusives of the Oaxaca complex in two small outliers northwest of Oaxaca City (Landing et al. 2007). These can be seen in the map in fig. 1.

The Tiñu Formation consists of two members, the lower Yudachica member and the upper Río Salinas member. They are distinguishable due to the fact that the lower part of the Tiñu Formation is very limestone-rich whilst the upper part is dominated by sandstones and shales. The age of the Tiñu Formation has been debated and correlated with several different successions around the world but has recently been determined by Landing et al. (2007) through a restudy of the conodont biostratigraphy and lithofacies in the unit. This study dates the Yudachica member to the upper part of the upper Cambrian and the Río Salinas member to the Lower Ordovician (Tremadoc) (Landing et al. 2007).

The source of the detritus in the Tiñu formation has been determined using geochemical and isotopic data and detrital age spectra. These methods together suggest that the underlying Oaxaca complex of 1 Ga is the source not only of the Tiñu Formation but very likely the source of the younger units as well (Gillis et al. 2005 and Murphy et al. 2005). See figs. 2 and 3 for sections and samples.

Yudachica member

The Yudachica member of the Tiñu Formation consists of interbedded medium grey limestones and light grey-brown, yellow-green weathering silt shales (Landing et al. 2007).

Río Salinas member

The lithologic contact between the Yudachica and the Río Salinas members in the Tiñu Formation is very sharp and marked by a limestone and silt-shale clast conglomerate. This conglomerate is thin and flat and is abruptly replaced upwards by organic-rich laminated shales with sideritic and pyrite nodules (Landing et al. 2007).

Description of the sampled localities

Locality Tu-

This locality is 59 km northwest of Oaxaca City, and is reached by exiting Federal Route MEX135 at Nochixtlán, driving 10 km south on Route 190 and thereafter driving 2 km west on the dirt road to Río Salinas village. Here the Tiñu Formation occurs in a NNE-trending and plunging syncline which is overlain by either Tertiary red beds or Cretaceous limestone on its east flank. The section is structurally simple, north dipping, 72 meters thick and lies just east of the synclinal axis of the formations type locality (Landing et al. 2007).

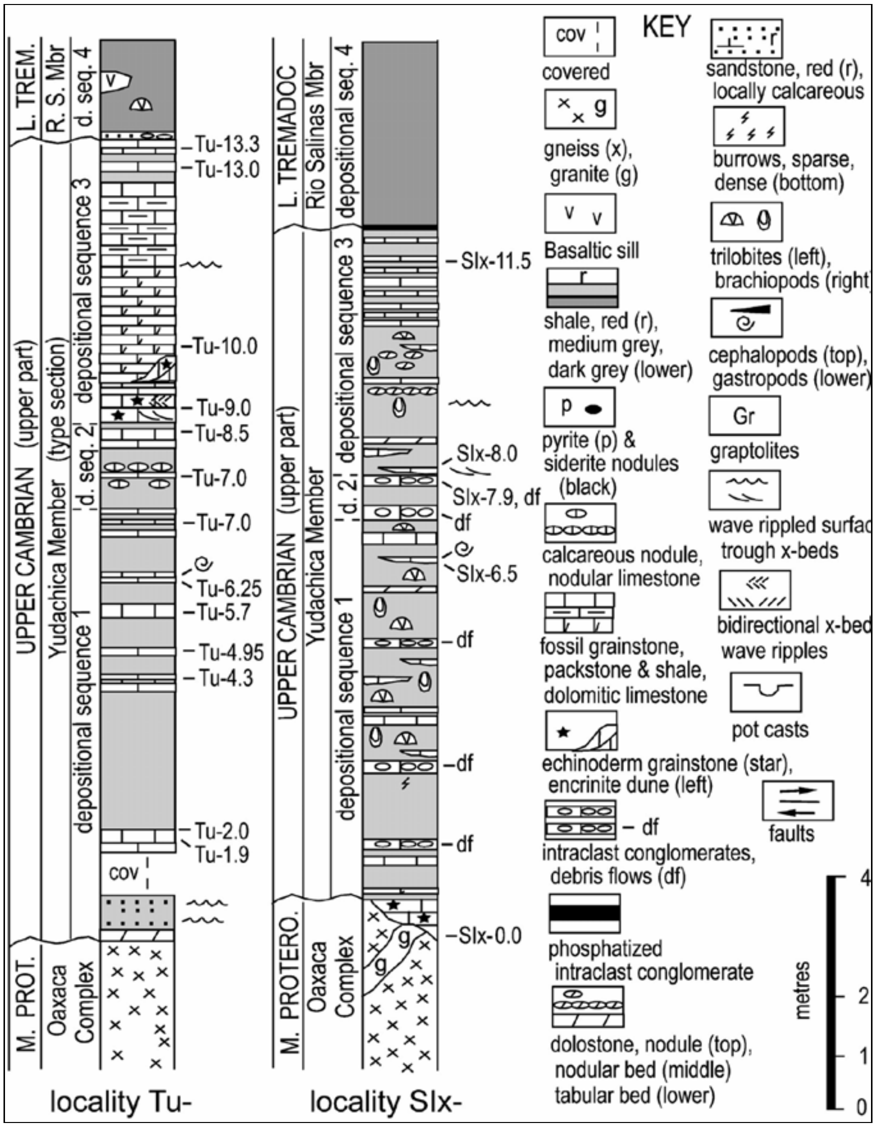

Fig. 2 Sections in the lower Tiñu Formation (Yudachica Member). Brachiopod samples SIx and Tu are indicated to the right of columns. The numbers after the locality abbreviation represent metres above the Oaxaca Complex. Figure shows proposed depositional sequences of Yudachica Member. (Fig. from Landing et al. 2007)

Locality Slx-

This locality is found 66 km northwest of Oaxaca City by driving 15.5 km on a dirt road northeast of Nochixtlán village and then just past the hair-pin curve north of Santiago Ixtaltepec hamlet. A path leads down the steeply east-dipping slope over the Carboniferous Ixtaltepec and Santiago formations north of Santiago Ixtaltepec village. The lower parts of the formation at this locality are structurally a rather simple section, dipping west. Higher in the formation the shales and sheared fine-grained sandstones have quartz vein intrusions, are faulted and folded and are, towards the contact with the Santiago formation, hydrothermally bleached (Landing et al. 2007).

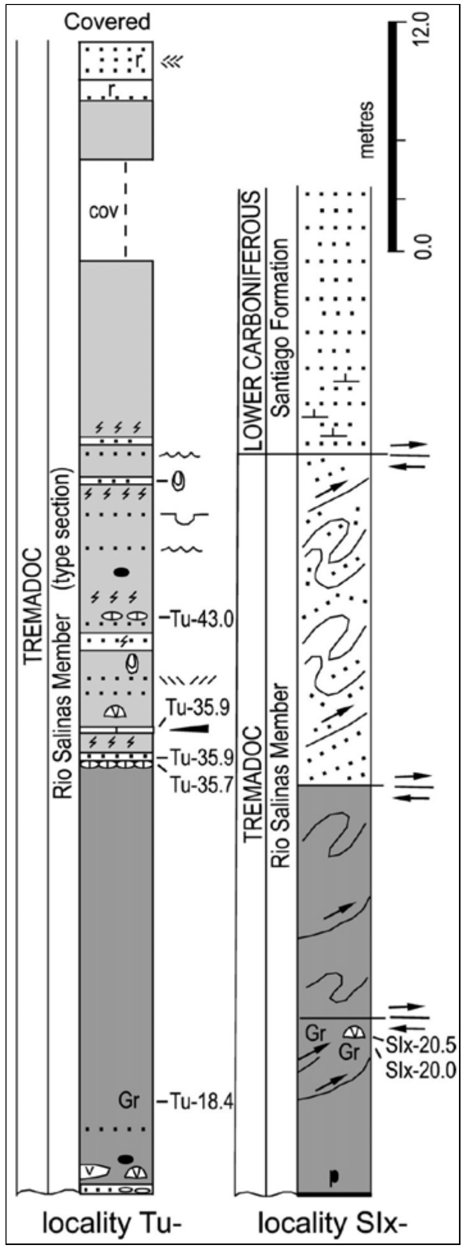

Fig. 3 Sections in the upper Tiñu Formation (Río Salinas Member). Samples (SIx and Tu) indicated to right of columns. Lithologies as in Figure 2. (Fig. from Landing et al. 2007).

Material and Methods

The material presented in this study was collected in Oaxaca State in southern Mexico as part of a larger study including the biotas and sequence stratigraphy of the Tiñu Formation (Landing et al. 2007). The collected rock samples (se figs. 2 and 3 for samples) were dissolved in diluted formic acid and the obtained residue was screened for fossils at the New York State Museum. Brachiopods found were sent to the Palaeobiology programme at Uppsala University for further analysis.

The specimens were examined under a stereomicroscope and representative specimens were coated with gold and thoroughly examined and photographed under a Scanning Electron Microscope (ZEISS Supra 35VP). The specimens were then identified to genus level and described.

Systematic palaeontology

Measurements (in µm) on valves are presented in the respective tables. Abbreviations: H, L, W = Height, Length and Width of valve; L_{mr} = Length median ridge to pseudointerarea; W_p = Width pseudointerarea; P = Pit diameter. Additional abbreviations: N = Number of specimens; MIN = minimum value of respective measurement; MAX = maximum value of respective measurement.

The species were called A-J during work and these letters have nothing to do with genus affinities.

Acrotretid brachiopods

The acrotretids found in the samples from the Tiñu Formation exhibit their very characteristic columnar shell structure (Holmer, 1989). They also display the cone-shaped ventral valves common among acrotretid brachiopods. Many acrotretids with cone-shaped ventral valves do have a high and branching median ridge on their dorsal valve, but this feature was only found in a few specimens in these samples.

Phylum **Brachiopda** (Duméril 1806)
Subphylum **Linguliformea** (Williams et al. 1996)
Class **Lingulata** (Gorjansky and Popov 1985)
Order **Acrotretida** (Kunh 1949)
Superfamily **Acrotretoidea** (Schuchert 1893)
Family **Acrotretidae** (Schuchert 1893)
Genus **Eurytreta** (Rowell 1966)
Species A:
Plates 1 and 2
Material studied: 10 ventral valves and 4 dorsal valves from two samples from the Yudachica member of the Tiñu Formation; Six – 0.0 and Tu – 1.9.
Applies to VV and DV: Shell ventribiconvex; the poorly preserved valves suggest a circular to transversely oval outline. The larval shell is ornamented with pits of usually uniform size and the transition from larval to post larval shell is gradual. Shell structure is columnar.
VV: The ventral valve is conical and the ventral pseudointerarea apsacline to catacline. An area with deviant structure is visible in the pseudointerarea. Foramen is enclosed in larval shell. Apical process is eroded but clearly visible and appear to be subtriangular.
DV: The studied dorsal valves are poorly preserved and incomplete. The dorsal pseudointerarea is characterized by a broad median groove bordered by laterally narrowing propareas. The median buttress is broad and connected to the low and slightly triangular median septum. The cardinal muscle scars are much eroded in all specimens but appear to be medium-sized, short, round to oval and relatively widely separated.

We had no complete specimens from which measurements could be obtained.

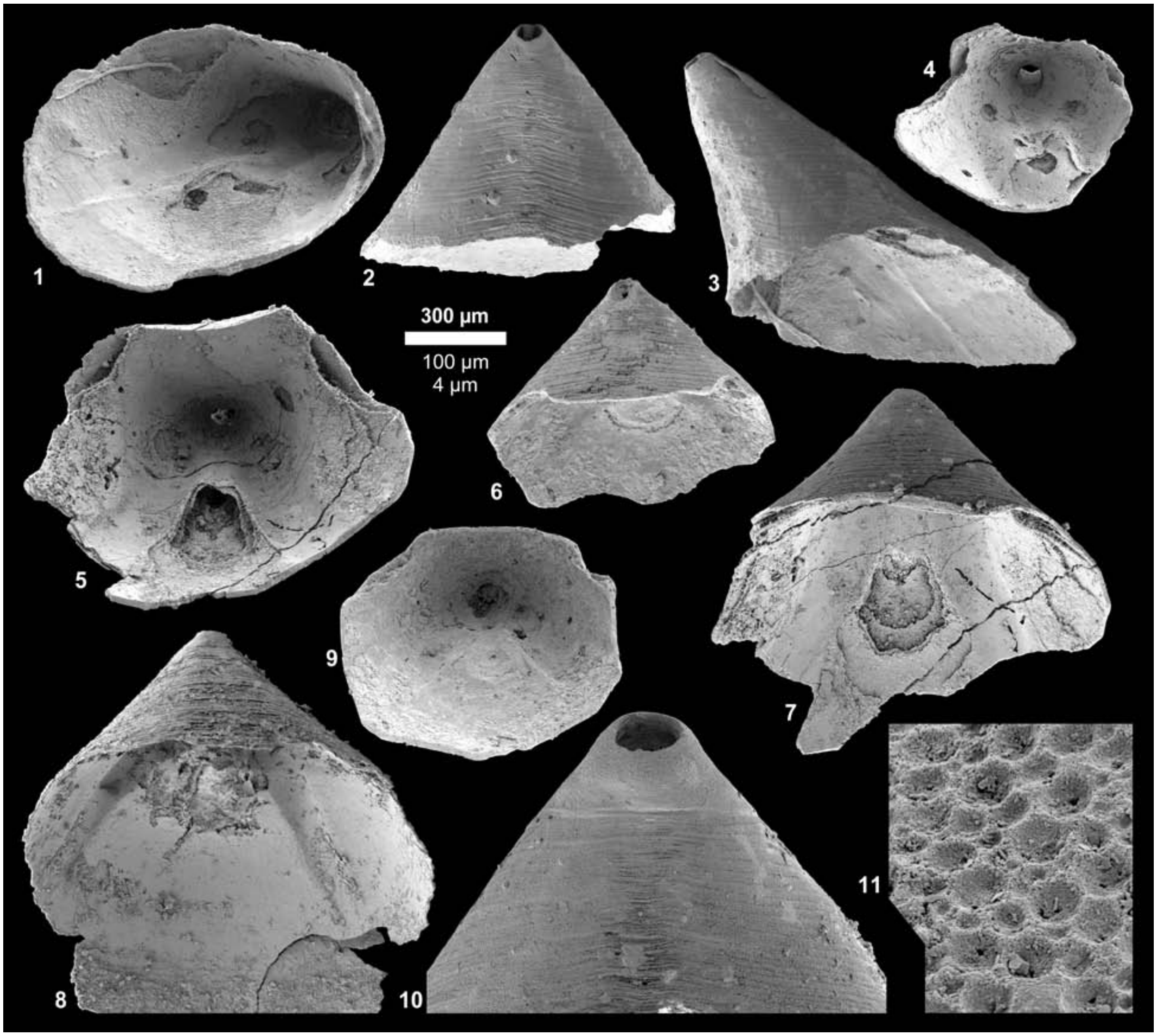

Plate 1. Species A. Ventral valves. Scale bar 300 µm for all pictures except 10 and 11.
1) BM1118b; Internal view.
2) BM1118e; External posterior view of pseudointerarea.
3) BM1118c; Lateral view.
4) BM1112a; Internal view.
5) BM1206d; Internal view.
6) BM1115a; External view of pseudointerarea.
7) BM1206a; Internal-external view.
8) BM1210; Internal-external view.
9) BM1115c; Internal view.
10) BM1112b; Close-up of pseudointerarea, larval shell and pedicle opening. Scale bar = 100 µm
11) BM1203d; Close-up of pitting on larval shell. Scale bar = 4 µm

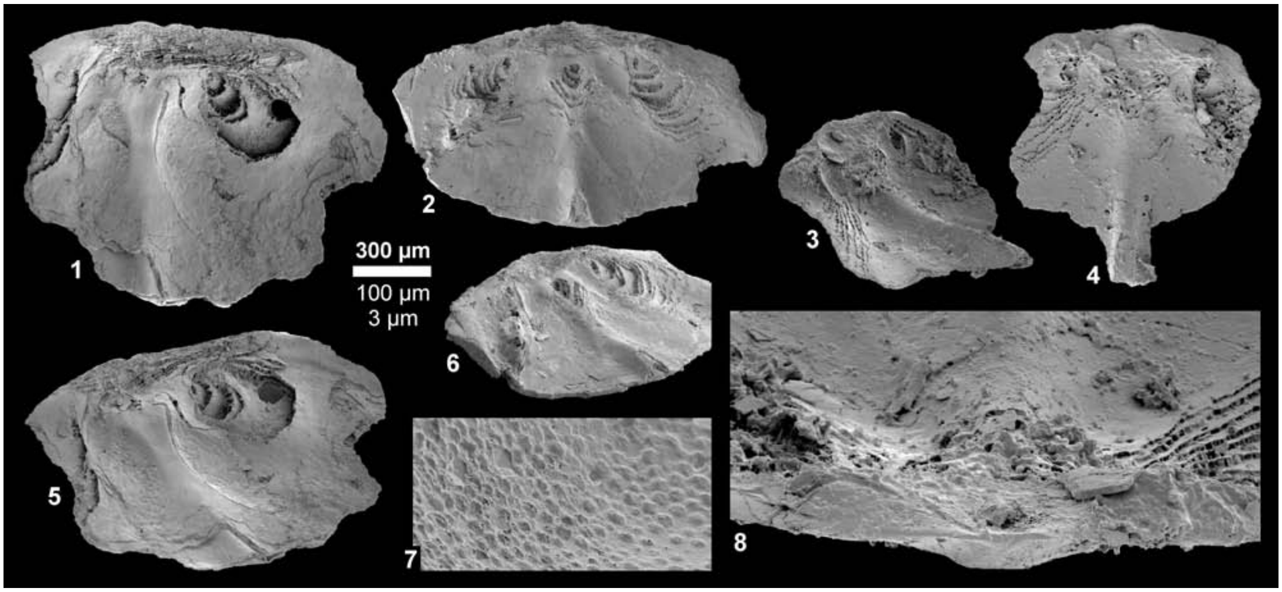

Plate 2. Species A. Dorsal valves. Scale bar 300 µm for all pictures except 7 and 8.
1) BM1207; interior view showing partial pseudointerarea and eroded cardinal muscle scars.
2) BM1117; interior view showing pseudointerarea, median buttress, median groove and eroded cardinal muscle scars.
3) BM1212; oblique view of interior showing median ridge.
4) BM1212d; interior view showing partial pseudointerarea, eroded cardinal muscle scars and a partial median ridge.
5) BM1207a; oblique view of interior.
6) BM1117b; oblique view of interior.
7) BM1212c; Close-up of pitting on larval shell. Scale bar = 3 µm
8) BM1212b; Close-up of pseudointerarea and median groove. Scale bar = 100 µm

Family **Acrotretidae** (Schuchert 1893)
Genus **Eurytreta** (Rowell 1966)
Species E
Plates 3, 4 (figs. 2-4 and 6-15) and 5
Material studied: 37 ventral valves and 9 dorsal valves from four samples from the Yudachica member of the Tiñu Formation; TU – 13.0, TU – 14.3, TU – 9.8 and TU – 8.5.
Applies to VV and DV: Shell ventribiconvex, the outline of the valve is typically circular, although a little wider than it is long. The maximum width occurs slightly anterior to midlength. The larval shell is ornamented with pits of usually uniform size, but they may also be of two different sizes in the same specimen, and the transition from larval to post-larval shell is gradual. The post-larval shell is characterized by concentric filae and sets of drapes. Shell structure is columnar.
VV: The ventral valve is subconical with an apsacline to catacline pseudointerarea. Intertrough is poorly defined. Pointy, almost tube shaped larval shell, foramen enclosed within larval shell. Larval shell ornamented with different-sized pits.
DV: The dorsal valve outline is typically circular, although occasionally slightly wider than it is long. It is pointed at the larval shell and which protrudes outside the post-larval shell. The valve is convex in lateral profile with its maximum height occurring posterior to midlength. Sulcus is present. The dorsal pseudointerarea is characterized by a broad triangular median groove bordered by laterally narrowing propareas. The median buttress is quite narrow and connected to the high and slim median septum almost as long as the valve length. The cardinal muscle scars are much eroded in all specimens but appear to be

medium-sized, not relatively widely separated and located posterior to midlength, not extending laterally to the pseudointerarea.

Table 1. Species E; measurements of ventral and dorsal valves. All measurements in µm.

Ventral valve	H	L	W	Lmr	Wp	P
N	0	0	0	0	0	2
MIN						1,75
MAX						2,22
MEAN						1,985

Dorsal valve	H	L	W	Lmr	Wp	P
N	0	2	3	1		1
MIN		1017	1106			
MAX		1338	1489			
MEAN		1177,5	1359,3	814		2,08

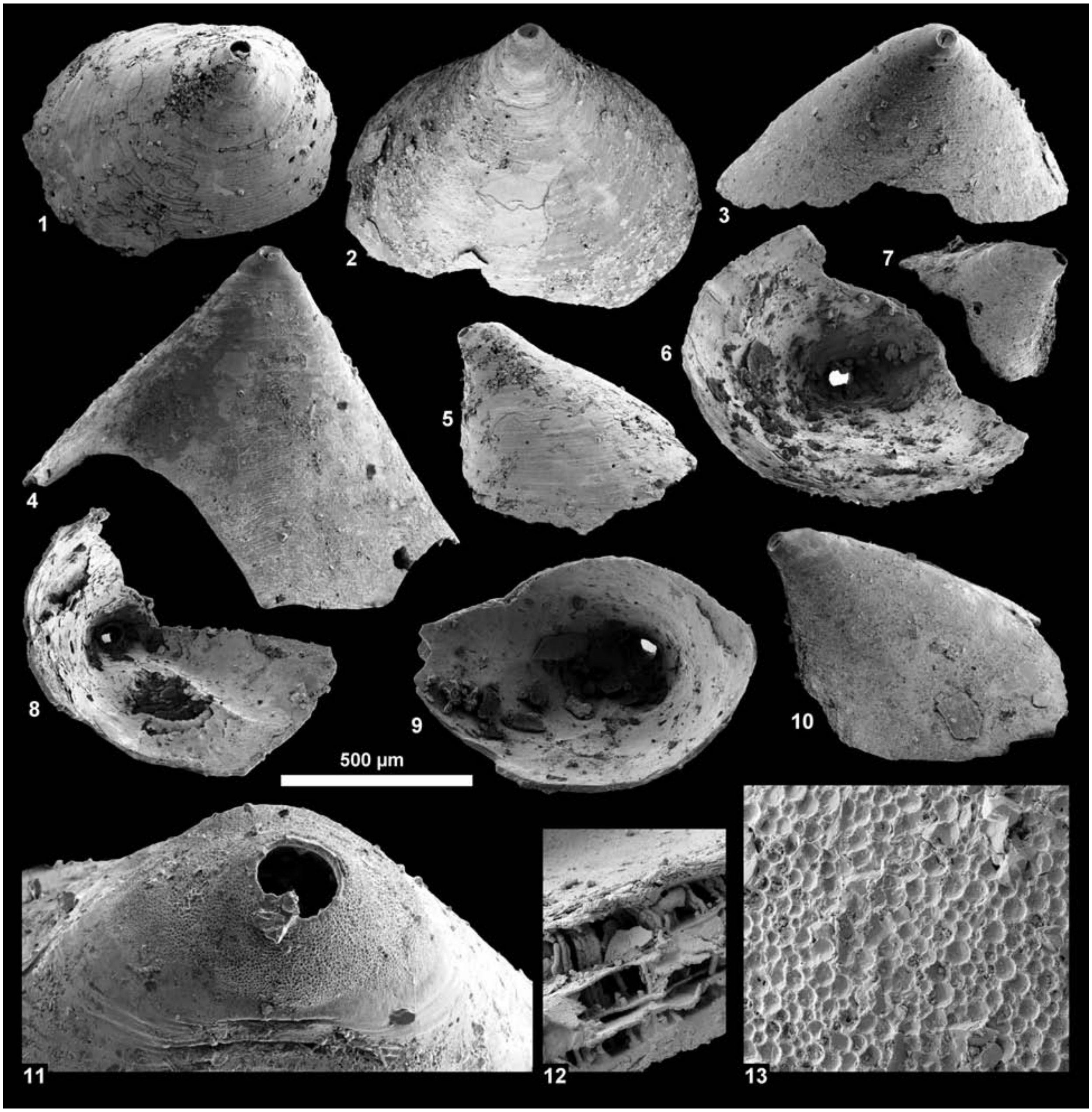

Plate 3. Species E. Ventral valves. Scale bar 500µm for all pictures except 11, 12 and 13.
1) BM315; Ventral exterior view.
2) BM720; Ventral oblique exterior view.
3) BM720e; Posterior exterior view.
4) BM709e; Posterior-lateral exterior view.
5) BM315; Lateral exterior view.
6) BM718f; Ventral interior view.
7) BM716f; Posterior exterior view.
8) BM708b; Ventral interior view.
9) BM705e; Ventral interior view.
10) BM720d; Lateral exterior view.
11) BM701e; Close-up of larval shell. Scale bar = 100 µm
12) BM708a; Close-up of columnar shell structure. Scale bar = 50 µm
13) BM701b; Close up of pitting on larval shell. Scale bar = 20 µ

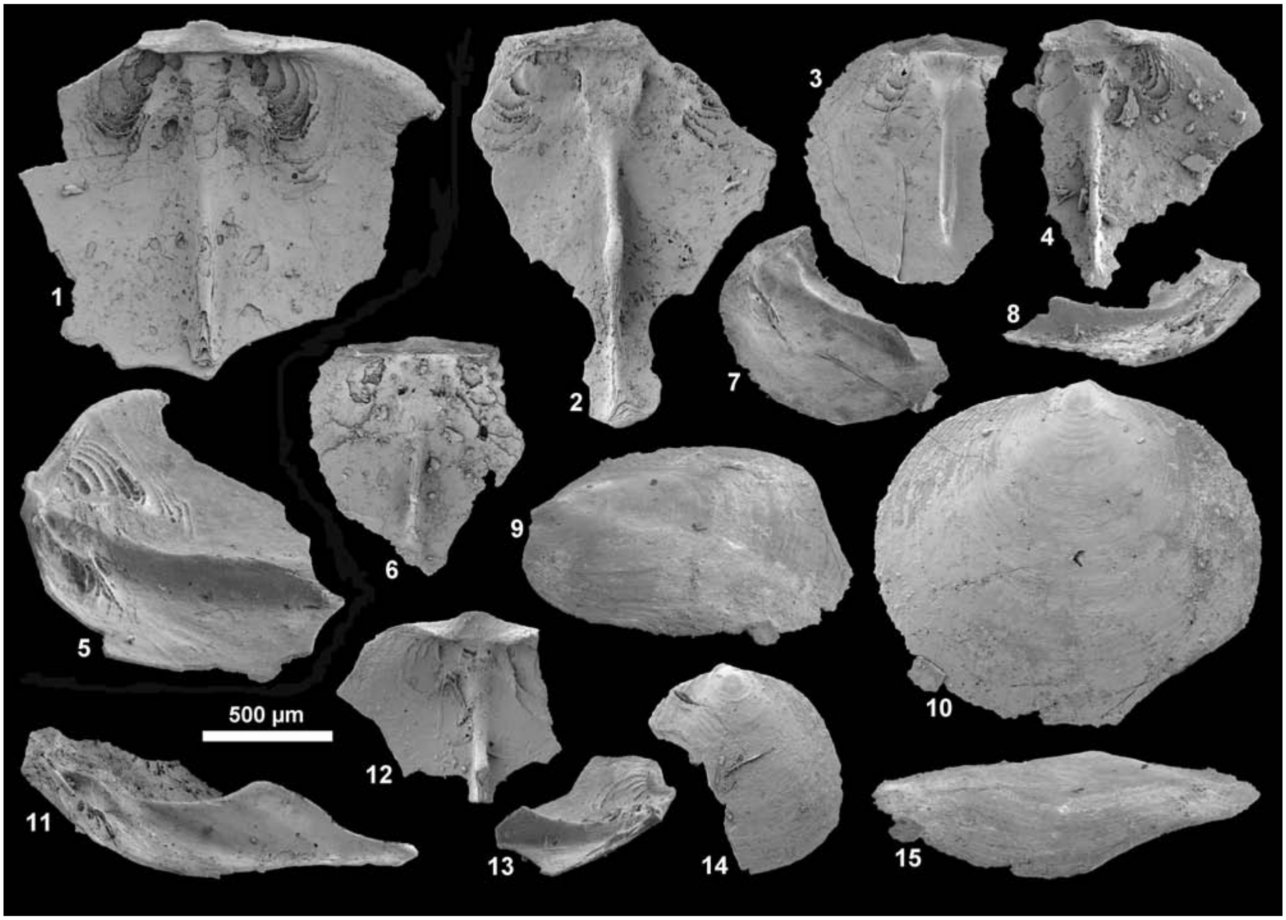

Plate 4. Species C (no. 1 and 5) and E (no. 2-4 and 6-15). Dorsal valves. Scale bar 500µm for all pictures.

1) BM1022 (species C); Dorsal interior view.
2) BM303a; Dorsal interior view.
3) BM1006; Dorsal interior view.
4) BM1002; Dorsal interior view.
5) BM1022b (species C); Oblique interior view.
6) BM710; Dorsal interior view.
7) BM1006b; Oblique interior view.
8) BM1002b; Lateral interior view showing the median septum.
9) BM1004f; Oblique exterior view.
10) BM1004; Dorsal exterior view.
11) BM303d; Lateral interior view showing the median septum.
12) BM1003; Dorsal interior view.
13) BM1003b; Oblique interior view.
14) BM1010: Dorsal exterior view.
15) BM1004e: Anterior exterior view.

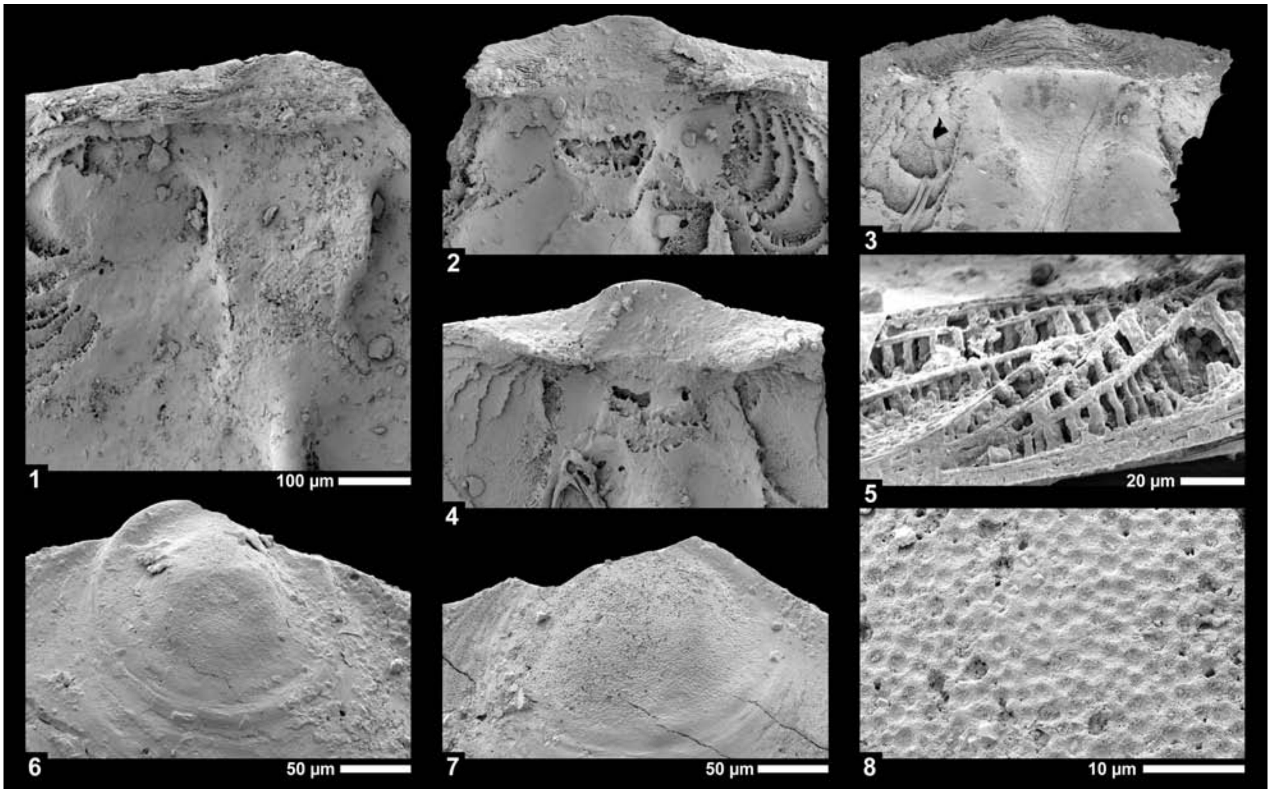

Plate 5. Species E. Dorsal valves. Scale bars as shown on plate.
1) BM303; Close-up showing median groove and median buttress.
2) BM1002a; Close-up showing median groove and median buttress.
3) BM1006a; Close-up showing median groove and median buttress.
4) BM1003a; Close-up showing median groove and median buttress.
5) BM303c; Close-up showing columnar shell structure.
6) BM1010a; Close-up of larval shell.
7) BM1004a: Close-up of larval shell.
8) BM1004b; Close-up of pitting on larval shell.

Family **Acrotretidae** (Schuchert 1893)
Genus **Eurytreta** (Rowell 1966)
Species C cf. species E:
Plate 4, (fig. 1 and 5)
Material studied: One dorsal valve from one sample from the Yudachica member of the Tiñu Formation; TU – 4.95
DV: The dorsal valve is pointed at the larval shell which protrudes outside the post-larval shell. The pseudointerarea is characterized by a broad median groove bordered by laterally narrowing propareas. The median buttress is very similar to Species E, but is slightly narrower and lacks its triangular shape. It is and connected to the high and slim median septum.
We had no complete specimens from which measurements could be obtained.

Family **Acrotretidae** (Schuchert 1893)
Genus **Eurytreta** (Rowell 1966)
Species H
Plates 6, 7 (fig. 2-14) and 8
Material studied: 11 ventral valves and 21 dorsal valves from one sample from the Río Salinas member of the Tiñu Formation; TU – 43.0.
Applies to VV and DV: Shell ventribiconvex, the outline of the valve is typically circular, although slightly wider than it is long. The maximum width occurs typically slightly anterior to midlength. The larval shell is ornamented with pits of usually uniform size and the transition

from larval to post larval shell is gradual. The post larval shell is characterized by concentric filae and sets of drapes. Shell structure is columnar.

VV: The ventral valve is subconical with an apsacline preudointerarea. Intertrough is poorly defined. Pointy, almost tube shaped larval shell, foramen enclosed within larval shell. Larval shell ornamented with uniformly-sized pits. Valve very narrow at larval shell and widens strongly towards the commissure.

DV: The dorsal valve outline is typically circular, although slightly wider than it is long and it has a rounded point at the larval shell which is protruding outside the post-larval shell. The valve is weakly convex in lateral profile with its maximum height occurring anterior to midlength. The dorsal pseudointerarea is characterized by a broad triangular median groove bordered by laterally narrowing propareas. The median buttress is poorly defined and connected to the low median septum which reaches ½ to 2/3 of the valve length. The cardinal muscle scars are very small and located close together.

Table 2. Species H; measurements of ventral and dorsal valves. All measurements in µm.

Ventral valve	H	L	W	Lmr	Wp	P
N	1		1			3
MIN						1,79
MAX						2,59
MEAN	835		1084			2,07

Dorsal valve	H	L	W	Lmr	Wp	P
N	0	11	12	2	4	5
MIN		670	735	651	297	1,34
MAX		1682	1788	1135	671	1,95
MEAN		986,727	1110,42	893	449	1,59

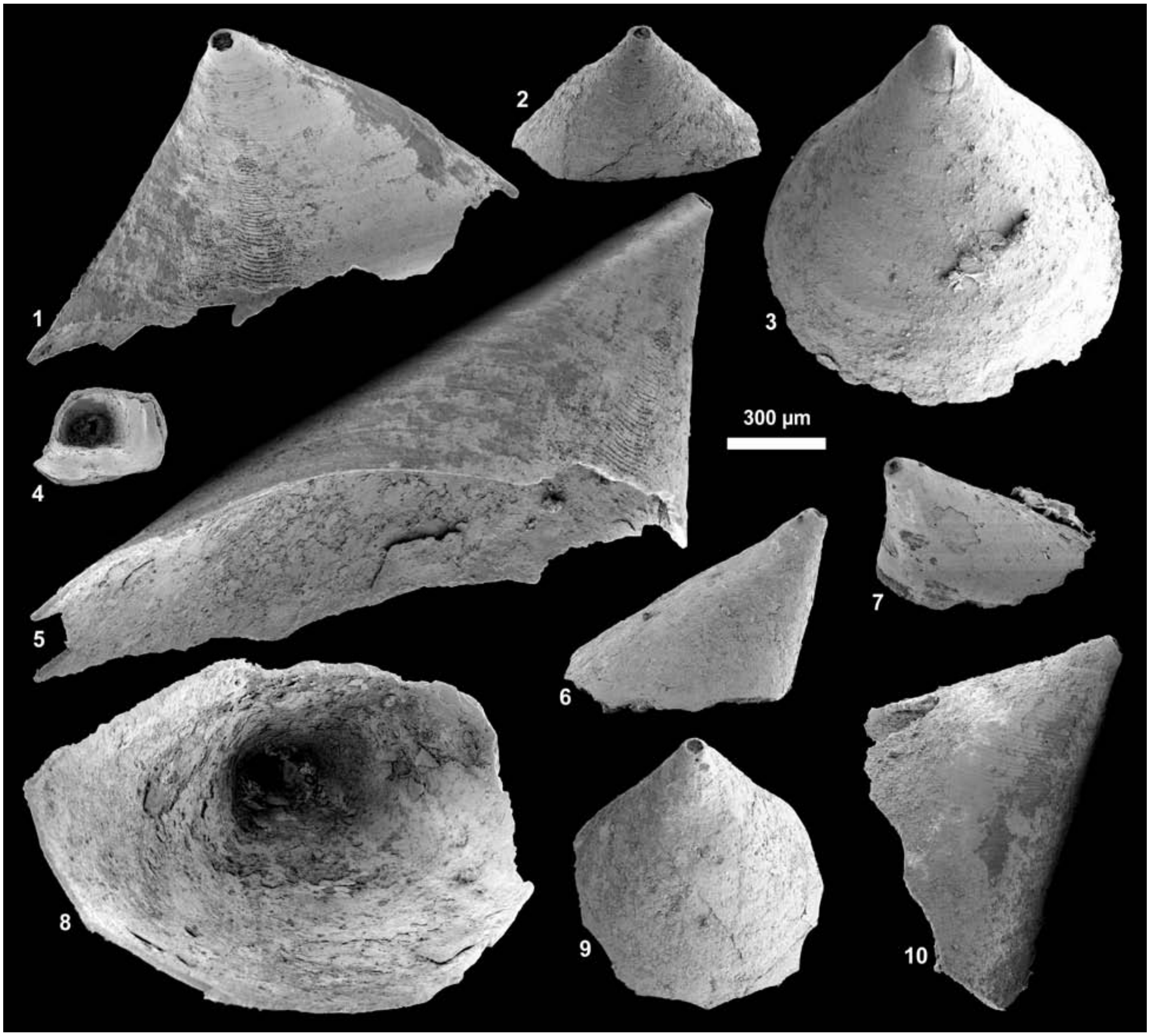

Plate 6. Species H. Ventral valves. Scale bar 300 µm in all pictures.
1) BM404g; Ventral oblique exterior view.
2) BM405c; Posterior exterior view.
3) BM406; Ventral exterior view.
4) BM419d; Ventral interior view.
5) BM404f; Lateral-posterior exterior view.
6) BM405b; Lateral exterior view.
7) BM420a; Lateral-posterior exterior view.
8) BM404e; Ventral interior view.
9) BM405; Ventral exterior view.
10) BM409b; Lateral exterior view.

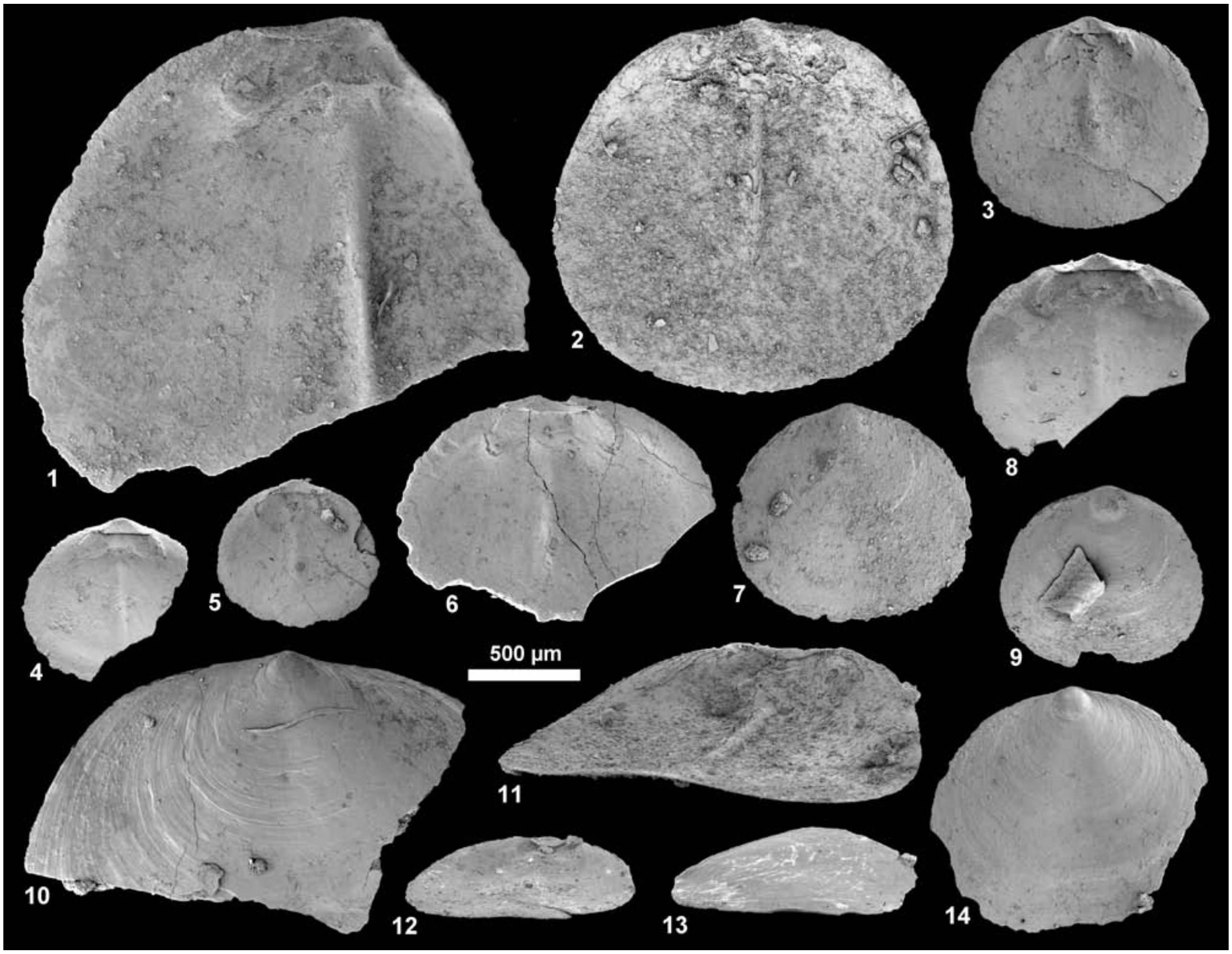

Plate 7. Species I (no. 1) and H (no. 2-14). Dorsal valves. Scale bar 500 µm for all pictures.
1) BM903 (species I); Dorsal interior view.
2) BM506; Dorsal interior view.
3) BM502; Dorsal interior view.
4) BM422; Dorsal interior view.
5) BM407; Dorsal interior view.
6) BM413; Dorsal interior view.
7) BM408; Dorsal exterior view.
8) BM421; Dorsal interior view.
9) BM424; Dorsal exterior view.
10) BM414; Dorsal exterior view.
11) BM506e; Oblique interior view.
12) BM502e; Oblique-anterior interior view.
13) BM401e; Lateral-oblique exterior view.
14) BM401; Dorsal exterior view.

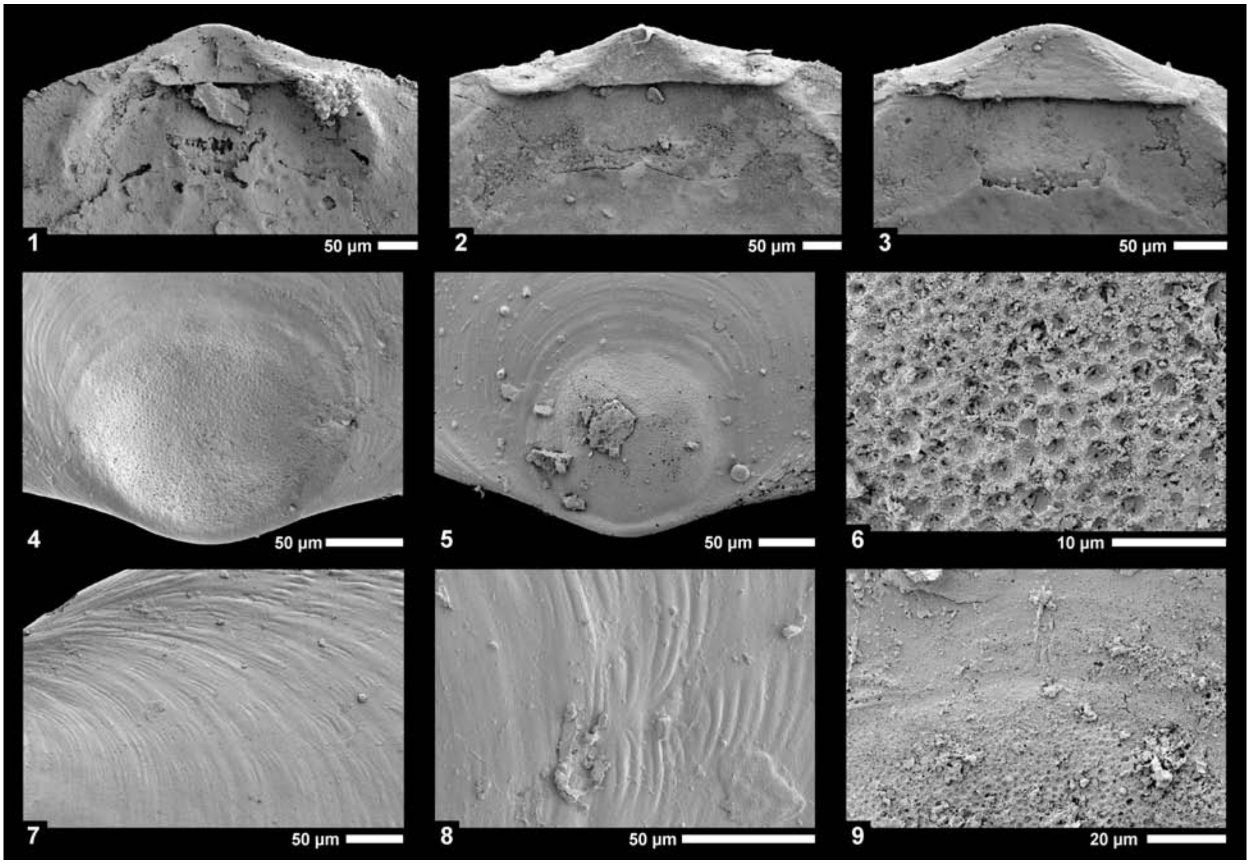

Plate 8. Species H. Dorsal valves. Scale bars as shown on plate.
1) BM502a; Close-up showing median groove and median buttress.
2) BM421a; Close-up showing median groove and median buttress.
3) BM422a; Close-up showing median groove and median buttress.
4) BM401a; Close-up of larval shell.
5) BM424a; Close-up of larval shell.
6) BM507b; Close-up of pitting on larval shell.
7) BM401d; Close-up of post-larval shell.
8) BM503e; Close-up of post-larval shell showing sets of drapes.
9) BM507c; Close-up of transition between post-larval and larval shell.

Family **Acrotretidae** (Schuchert 1893)
Genus **Eurytreta** (Rowell 1966)
Species I: Acrotretids
Plates 7 (fig. 1) and 9
Material studied: One dorsal valve and 16 ventral valves from two samples from the Río Salinas member of the Tiñu Formation; TU – 35.7 and 35.9.
Applies to VV and DV: Shell ventribiconvex, the outline of the valves appear to be circular, but the specimens are poorly preserved which makes confirmation of this impossible. The larval shell is ornamented with pits of usually uniform size and the transition from larval to post larval shell is gradual. Shell structure is columnar.
VV: The ventral valve is subconical with an apsacline pseudointerarea. The pseudointerarea is concave in lateral view and has a triangular area widening dorsally flanked by two depressions.
Very tube shaped larval shell, foramen enclosed within larval shell. Larval shell ornamented with pits of uniform size. Valve very narrow at larval shell and widens strongly dorsally.
DV: The dorsal valve outline is most likely circular. The dorsal pseudointerarea is characterized by a triangular median

groove bordered by laterally narrowing propareas. The median buttress is poorly defined and connected to the low and thin median septum. The cardinal muscle scars are very small and located close together.

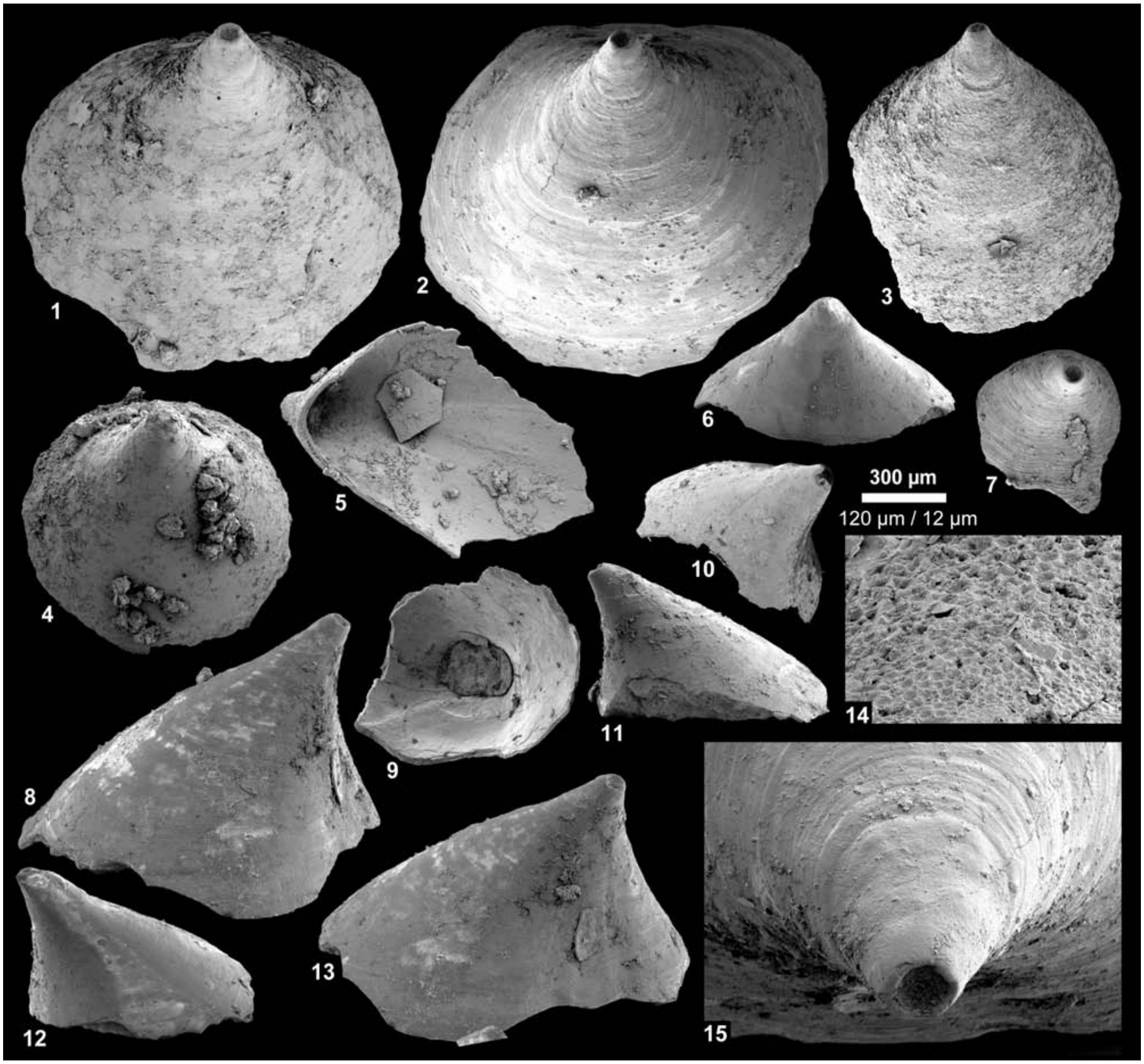

Plate 9. Species I. Ventral valves. Scale bar 300 µm in all pictures except 14 and 15.
1) BM617a; Ventral exterior view.
2) BM609; Ventral exterior view.
3) BM604; Ventral exterior view.
4) BM608a; Ventral exterior view.
5) BM603; Oblique interior view.
6) BM605c; Posterior exterior view.
7) BM614a; Ventral exterior view.
8) BM609c; Lateral exterior view.
9) BM601c; Ventral interior view.
10) BM601e; Ventral exterior view.
11) BM602d; Lateral exterior view.

12) BM605b; Lateral exterior view.
13) BM609b; Oblique exterior view.
14) BM603c; Close-up of pitting on larval shell. Scale bar = 12 µm
15) BM609a; Close-up of larval shell. Scale bar = 120 µm

Family **Acrotretidae** (Schuchert 1893)
Genus cf. **Eurytreta** (Rowell 1966)
Species J: Acrotretids
Plate 10
Material studied: Six ventral valves from one sample from the Río Salinas member of the Tiñu Formation; TU – 43.0.

VV: The ventral valve is very conical and narrow but appears to widen dorsally, but all specimens have been broken off so this is difficult to confirm. Intertrough is poorly defined. Larval shell ornamented with pits of different sizes.

We had no complete specimens from which measurements could be obtained.

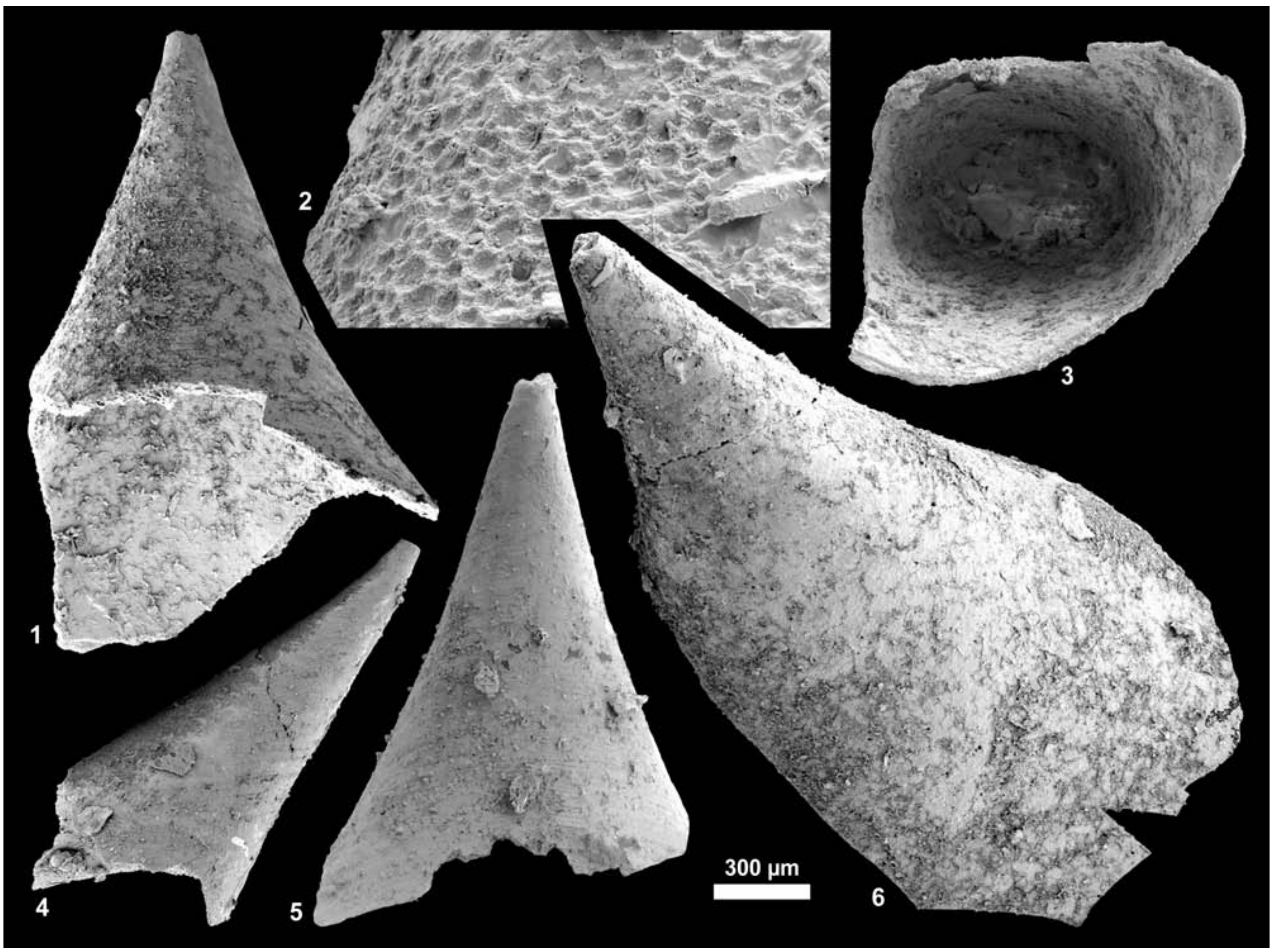

Plate 10. Species J. Ventral valves. Scale bar 300 µm in all pictures except 2.
1) BM511a; Lateral exterior view.
2) BM403b; Close-up of pitting on larval shell. Scale bar = 6 µm
3) BM511g; Ventral interior view.
4) BM403c; Lateral exterior view.
5) BM520b; Lateral exterior view.
6) BM509; Ventral exterior view.

Family **Acrotretidae** (Schuchert 1893)
Genus **Neotreta** (Sobolev 1976)
Species B:
Plate 11
Material studied: One dorsal valve from one sample from the Yudachica member of the Tiñu Formation; TU – 2.05

DV: Shell likely to be biconvex, transversely oval with wide, straight posterior margin. The larval shell is ornamented with pitting where the pits vary in size.

We had no complete specimens from which measurements could be obtained.

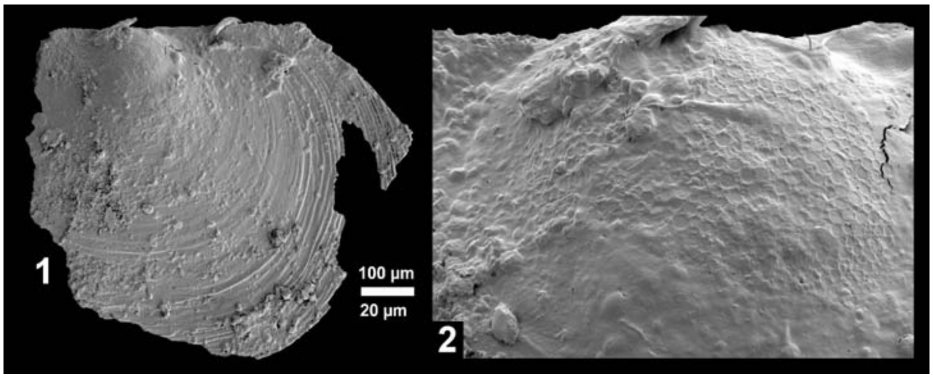

Plate 11. Species B. Dorsal valve. Scale bar 100 µm in picture 1 and 20µm in picture 2.
1) BM1202; exterior view
2) BM1202a; Close-up of larval shell with pitting.

Family **Acrotretidae** (Schuchert 1893)
Genus **Treptotreta?** (Henderson & MacKinnon 1981)
Species G
Plate 12
Material studied: One ventral valve from one sample from the Yudachica member of the Tiñu Formation; TU – 5.7
VV: Ventral valve conical. Very eroded interiorly, but the clearly visible cardinal muscle scars are small and placed widely apart. Apical process and vascula lateralia strongly defined. The apical process may widen posteriorly. The shell structure is columnar and the shell has been exfoliated, displaying other structures like septa.

We had no complete specimens from which measurements could be obtained.

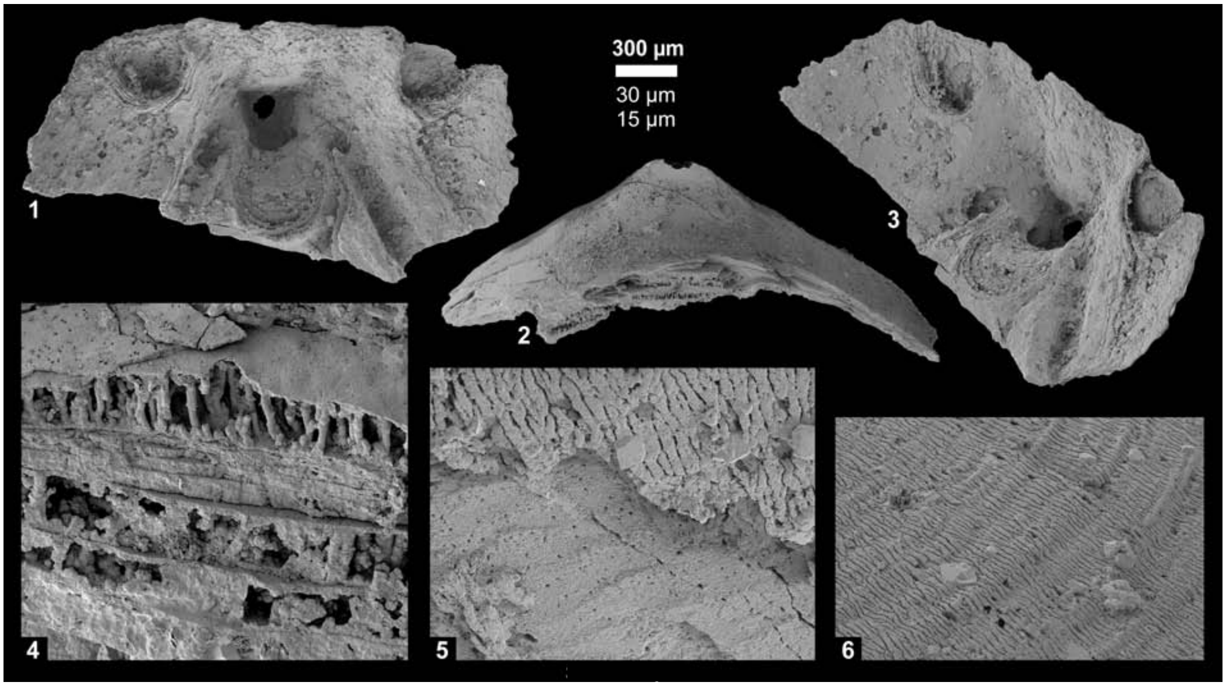

Plate 12. Species G. Scale bar 300 µm for all pictures except 4, 5 and 6.
1) BM809L; Interior view.
2) BM809O; Exterior view.
3) BM809M; Interior view.
4) BM809b; Close-up of columnar shell structure. Scale bar = 30 µm
5) BM809h; Close-up of surface structure. Scale bar = 15 µm
6) BM809i; Close-up of surface structure. Scale bar = 30 µm

Family **Ceratretidae** (Rowell 1965)
Genus **Uncertain**
Species D:
Plates 13, 14 and 15
Material studied: Six ventral valves (VV) and 32 dorsal valves (DV) from one sample (Tu-5.7) from the Yudachica member of the Tiñu Formation.
Applies to VV and DV: Shell ventribiconvex, outline nearly circular to slightly transversely oval, maximum width occurs at midlength. The larval shell is ornamented with circular pits of fairly equal size; the transition from larval shell to post-larval shell is gradual. Post larval shell is characterized by concentric filae and sets of drapes. The shell has a columnar structure.
VV: The ventral valve outline is transversely oval and has a procline to catacline pseudointerarea. Poorly defined intertrough and propareas. Large circular foramen enclosed in the larval shell.
DV: The dorsal valve is circular to transversely oval in outline and is convex in a lateral view, with its maximum height occurring at midlength. Interiorly the dorsal valve has a pseudointerarea with a fairly broad median groove, the median buttress is distinct and of a triangular shape and is connected to the medium-thick median septum, which stretches almost the full length of the valve and is bulbous at its highest point. The cardinal muscle scars are close together and anterolateral to the median groove. They are kidney shaped.

Table 3. Species D; measurements of ventral and dorsal valves. All measurements in µm.

Ventral valve	H	L	W	Lmr	Wp	P
N	3	3	3			1
MIN	338	437	579			
MAX	1155	950	1495			
MEAN	809	771,667	1154			1,86

Dorsal valve	H	L	W	Lmr	Wp	P
N	2	30	30	18	17	7
MIN	389	553	704	397	292	1,17
MAX	451	1395	1769	1142	1027	1,86
MEAN	420	1074,17	1379,1	846,278	709,353	1,54714

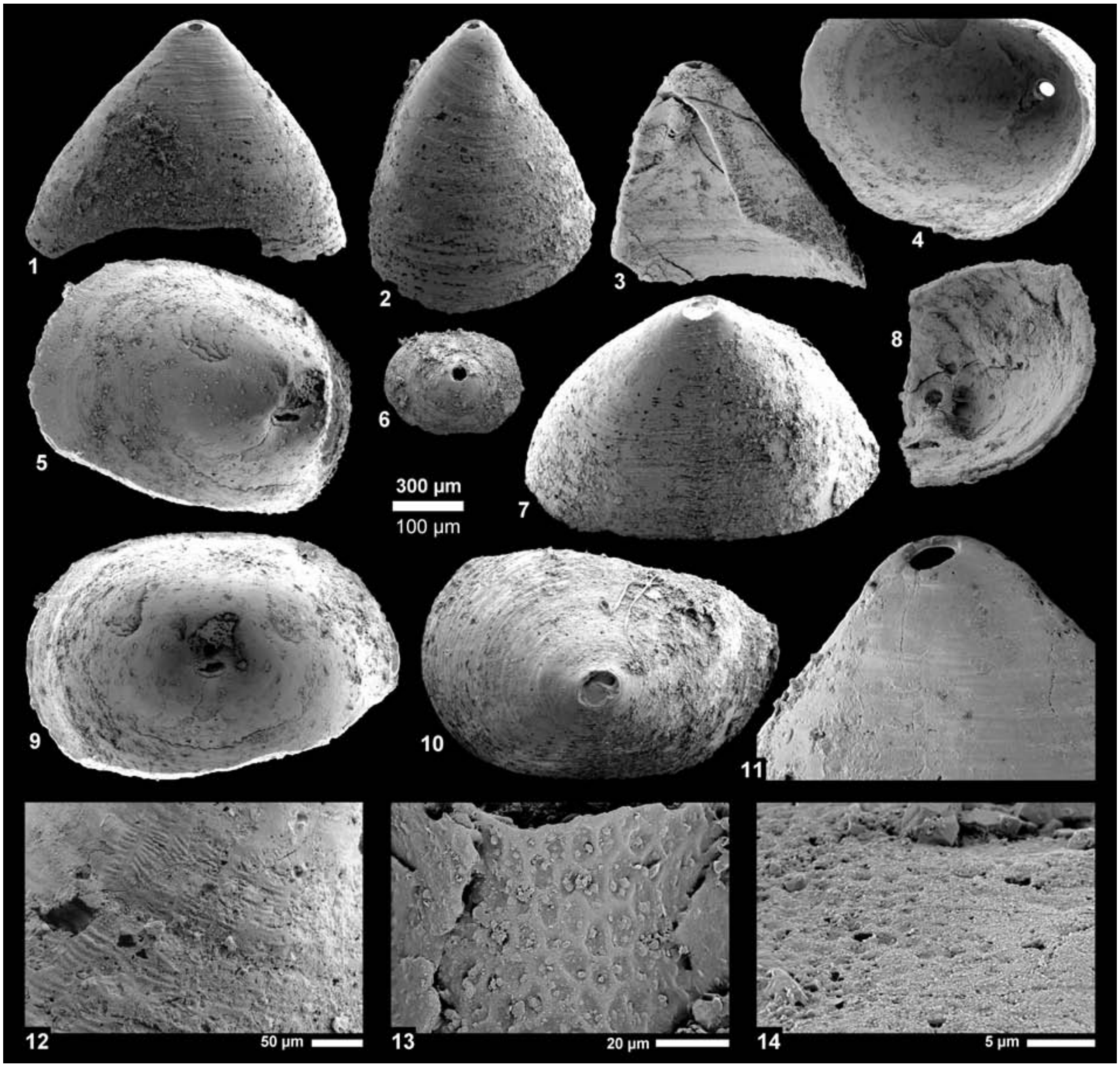

Plate 13. Species D. Ventral valves. Scale bar 300 µm for all pictures except 11, 12, 13 and 14.
1) BM205c; External posterior view.
2) BM205b; External lateral profile.
3) BM0104N; External-internal lateral profile.
4) BM205L; Internal view.
5) BM 0103J; Oblique view of interior.
6) BM210b; Ventral view.
7) BM103c; External posterior view.
8) BM0104; Internal view.
9) BM0103H; Internal view.
10) BM103d; Ventral view.
11) BM205N; Close-up of larval shell. Scale bar = 100 µm
12) BM205a; Close-up of set of drapes. Scale bar = 50 µm
13) BM0103I; Close-up of epithelial imprints. Scale bar = 20 µm
14) BM0104J; Close-up of pitting on larval shell. Scale bar = 5 µm

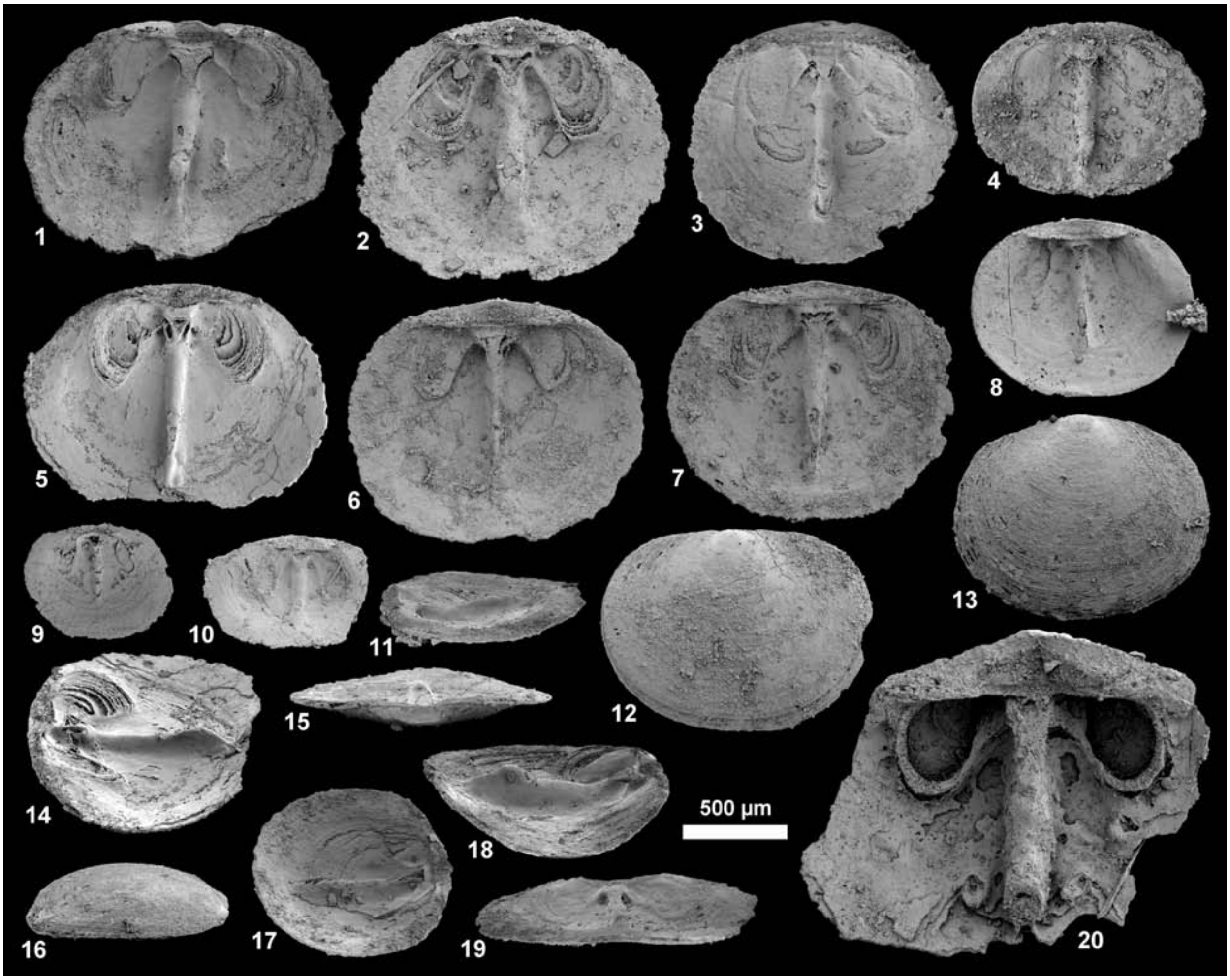

Plate 14. Species D. Dorsal valves. Scale bar 500 µm for all pictures.
1) BM105b; Dorsal interior view.
2) BM815; Dorsal interior view.
3) BM820; Dorsal interior view.
4) BM212b; Dorsal interior view.
5) BM206; Dorsal interior view.
6) BM812; Dorsal interior view.
7) BM810; Dorsal interior view.
8) BM 822; Dorsal interior view.
9) BM209a; Dorsal interior view.
10) BM816; Dorsal interior view.
11) BM802c; Oblique interior view.
12) BM811; Exterior view.
13) BM102; Exterior view.
14) BM206a; Oblique interior view.
15) BM803d; Posterior interior view.
16) BM102d; Oblique exterior view.
17) BM204b; Oblique interior view.
18) BM105; Oblique interior view.
19) BM802b; Anterior interior view.
20) BM805; Dorsal interior view.

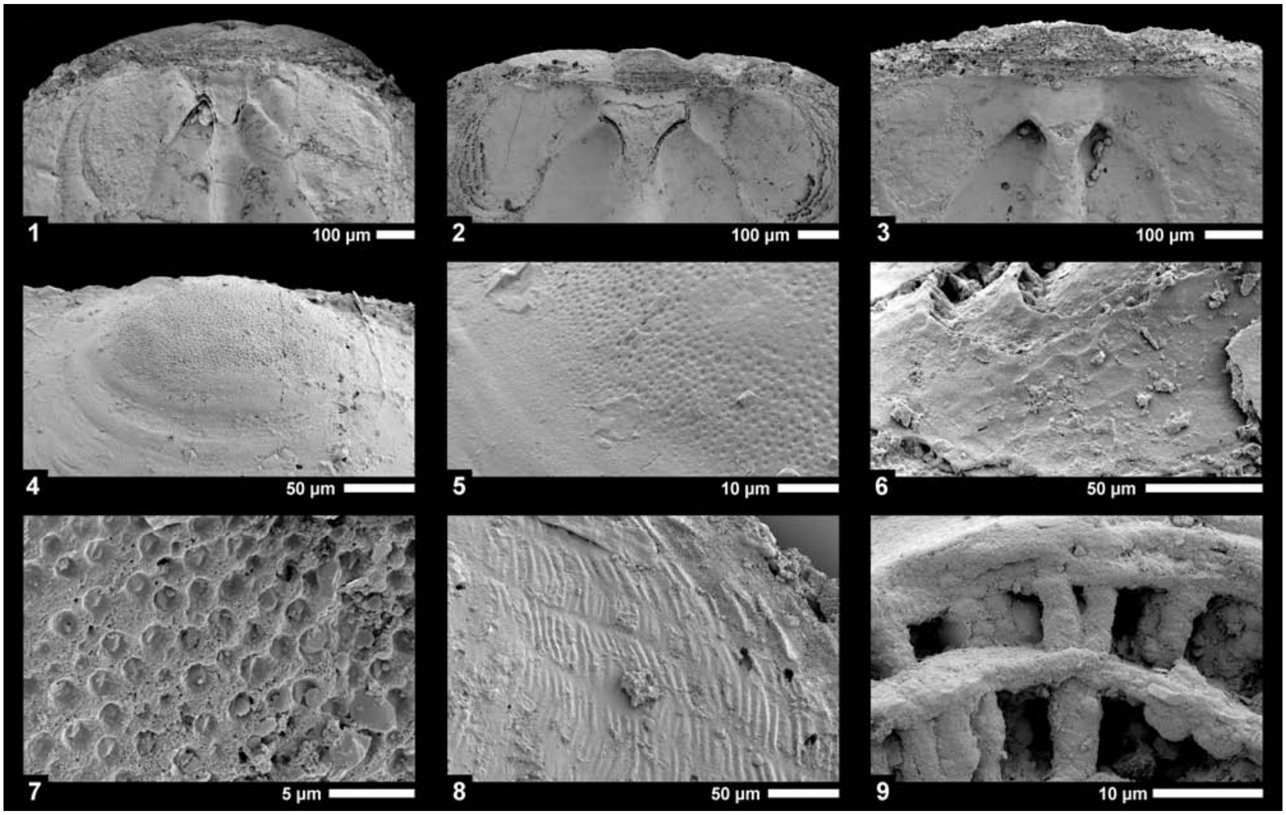

Plate 15. Species D. Scale bars as shown in plate.
1) BM820a; Close-up of pseudointerarea, median buttress and cardinal muscle scars.
2) BM105e; Close-up of pseudointerarea, median buttress and cardinal muscle scars.
3) BM802a; Close-up of pseudointerarea, median buttress and cardinal muscle scars.
4) BM821a; Close-up of larval shell.
5) BM811c; Close-up of transition between larval and post-larval shell.
6) BM204a; Close-up of epithelial imprints.
7) BM803f; Close-up of pitting on larval shell.
8) BM821e; Close-up of sets of drapes on post-larval shell.
9) BM08XXX; Close-up of columnar shell structure.

Siphonotretid brachiopods

Siphonotretid brachiopods are a species-poor group that is comparatively little known. They have a very characteristic pedicle foramen with a pedicle track area, which grows and changes shape through resorption during the lifetime of the brachiopod. The pedicle opening is usually shaped like a drop or an egg.

Phylum **Brachiopda** (Duméril 1806)
Subphylum **Linguliformea** (Williams et al. 1996)
Class **Lingulata** (Gorjansky and Popov 1985)
Order **Siphonotretida** (Kuhn 1949)
Superfamily **Siphonotretoidea** (Kutorga 1848)
Family **Siphonotretidae** (Kutorga 1848)
Genus **Schizambon** (Walcott 1884)

Species F

Plates 16 and 17
Material studied: 12 ventral valves and 2 dorsal valves from four samples from the Yudachica and the Río Salinas members of the Tiñu Formation; TU – 5.7, TU – 8.5, TU - 13.0 and TU – 14.3
Applies to VV and DV: Shell ventribiconvex, ornamented with rugellae and costellae. No spines visible. Visceral areas slightly thickened.
VV: Ventral valve pseudointerarea is procline. The pedicle track is elongate to triangular. The foramen is surrounded by a pair of “lips” or “wings” protruding from the valve. These vary from being quite low and small to being high and wide.
DV: Dorsal valve pseudointerarea low, with a poorly defined median groove.

We had no complete specimens from which measurements could be obtained.

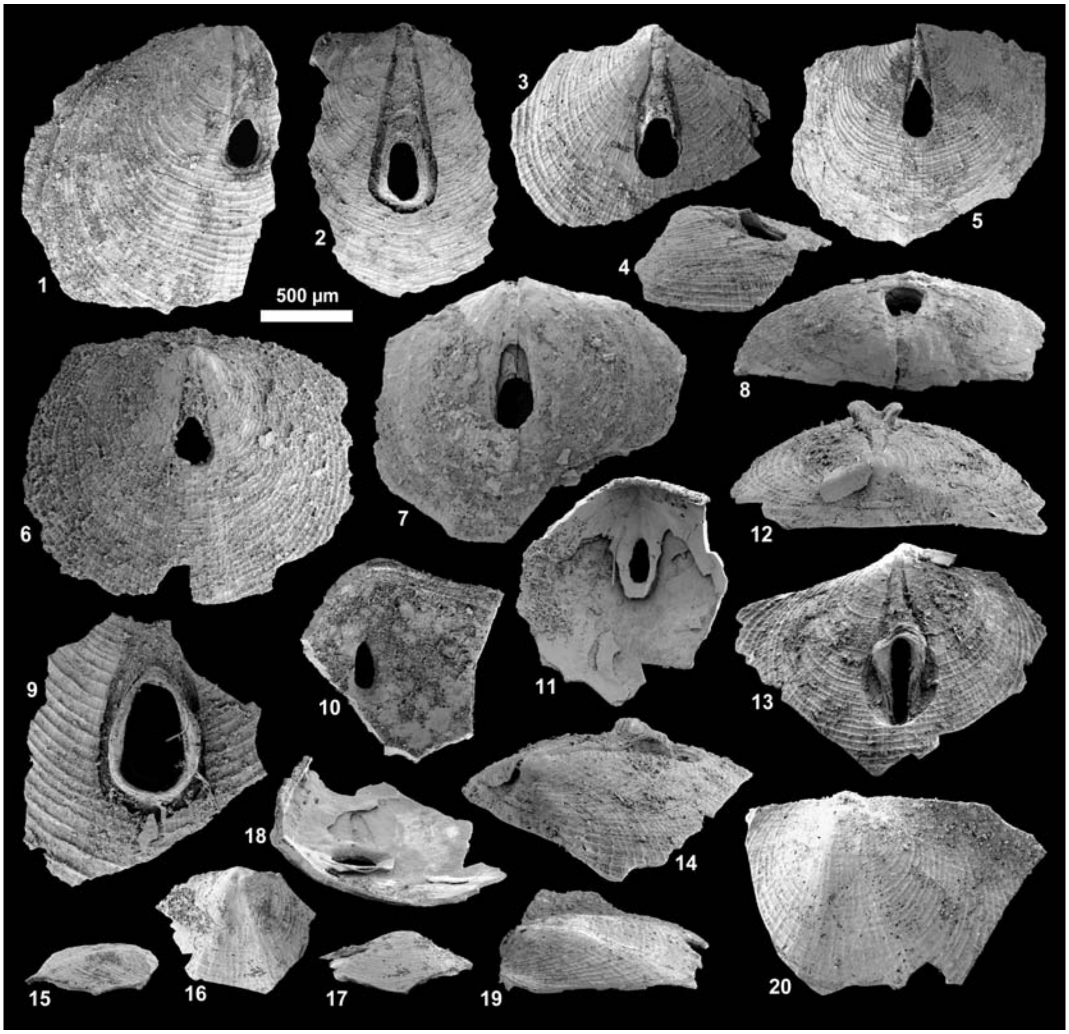

Plate 16. Species F. Scale bar 500 µm for all pictures.
1) BM302; Ventral exterior view of ventral valve.
2) BM203; Ventral exterior view of ventral valve.
3) BM306; Ventral exterior view of ventral valve.
4) BM306d; Oblique external view of ventral valve.
5) BM309; Ventral exterior view of ventral valve.
6) BM702; Ventral exterior view of ventral valve.
7) BM1108c; Ventral exterior view of ventral valve.
8) BM1108; Posterior external view of ventral valve.
9) BM201; Ventral exterior view of ventral valve.
10) BM307; Ventral internal view of ventral valve.
11) BM301; Ventral internal view of ventral valve.
12) BM0202N; Posterior external view of ventral valve.
13) BM202b; Anterior exterior view of ventral valve.
14) BM0202O; Lateral-posterior external view of ventral valve.
15) BM312c; Lateral view of dorsal valve.
16) BM312; Dorsal view of dorsal valve.
17) BM312d; Anterior exterior view of dorsal valve.
18) BM301a; Oblique internal view of ventral valve.
19) BM305c; Lateral external view of dorsal valve.
20) BM305; Dorsal external view of dorsal valve.

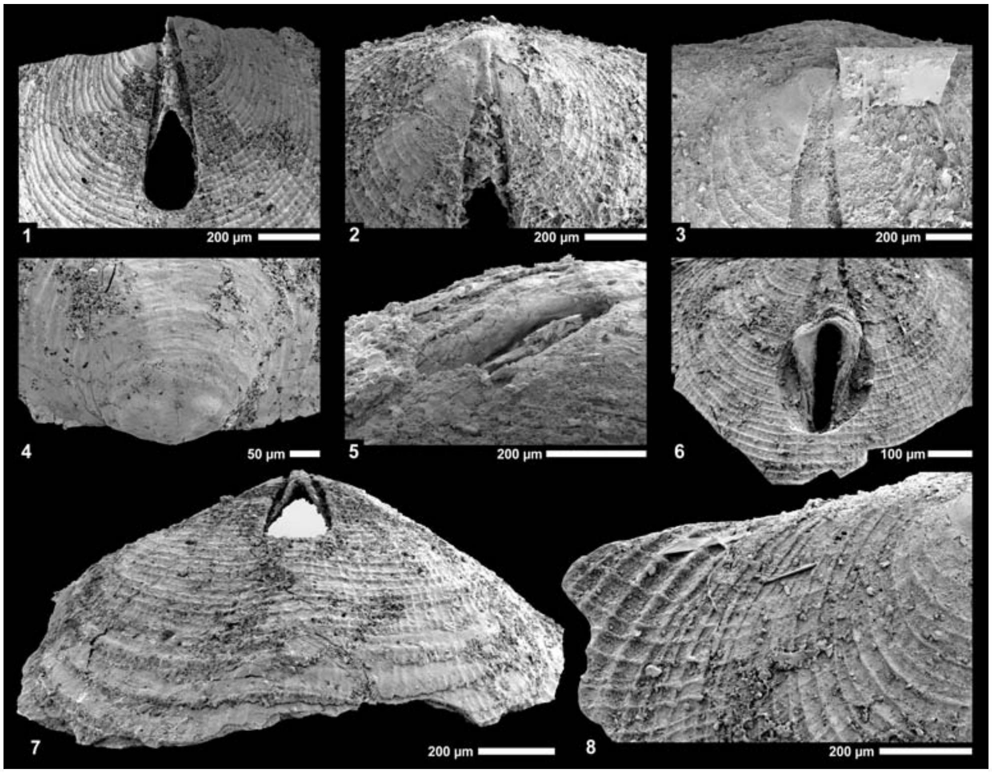

Plate 17. Species F. Scale bars as indicated in pictures.
1) BM309c; Close-up of pedicle opening and pedicle track.
2) BM308a; Close-up of larval shell, pedicle opening and pedicle track.
3) BM0202K; Close-up of larval shell and pedicle track.
4) BM312a; Close-up of larval shell.
5) BM1108a; Close-up of pedicle opening.
6) BM202c; Close-up of pedicle opening.
7) BM309d; Anterior exterior view.
8) BM202a; Close-up of shell ornamentation.

Other fossils

A few orthid brachiopods were found in the Tiñu Formation samples and all of the specimens are internal moulds. They all display a beautiful fish scale-like ornamentation over the entire surface of the mould but this is most likely not a primary structure, but has appeared due to re-mineralization. A small number of Lingulid brachiopods were also found.

Given that my samples were previously screened at New York State Museum, they contained few fossils other than those mentioned above. The only non-brachiopod fossils found were a few phospatocopines and a couple of trilobite fragments.

Discussion

The five species of Eurytretids that have been identified in this study are, at first glance, very similar. Various morphological features have been used to separate them. One of those features is the median septum on the dorsal valve. Species A has a very low and triangular median septum, which does not occur in any of the other eurytretids described. Species E and C are very similar but Sp. E has a very high and slender median septum whilst Sp. C's septum can be described as slim and subtriangular. Species H has a septum which is so low that it is barely visible. This also applies to Sp. I. The size, shape and placement of the cardinal muscle scars on the dorsal valves have also been very useful for differentiating the species. In Species A, the muscle scars are medium-sized, round to oval and fairly widely separated. In Species H and I, they are very small and placed very closely together. Also the shape and placement of the larval shell has been used as a classification feature. In Sp. A, no part of the larval shell can be seen from an interior view but in Sp. C, E and H the larval shell protrudes like a tip over the median groove. Sp. E and H also display differently shaped larval shells: in E it is completely circular and looks like it has been placed on top of the post-larval shell, whilst in Sp. I it appears to be enclosed in the post-larval shell and is more circular-to-oval.

The ventral valves reveal further species-typical differences. Sp. A has a rounded larval shell with a large circular pedicle opening. In Sp. E and H, the larval shell is much less rounded and appreciably more tubular. In Sp. I it definitely looks like a tube and is not rounded at a ll. The shape of the ventral valve itself also varies quite a lot, from the rather wide valves seen in Sp. H and I to the very pointy valves exhibited in Sp. J.

The siphonotretid species, *Schizambon sp. F* possesses some features that differentiate it from other siphonotretids and particularly from the Schizambon already described. One of these features is its complete lack of spines, which is a otherwise common siphonotretid feature. The “lips” or “wings” surrounding the pedicle opening are not found in any other siphonotretid which quite clearly indicates that this is a new species.

Conclusions

In total, ten linguliform brachiopod species were found in the Tiñu Formation material. These were sorted into two orders, Acrotretida and Siphonotretida, and thereafter further assigned to families. Eight of the species belong in the family Acrotretidae, one in the family Ceratretidae and one in the family Siphonotretidae. The brachiopods studied were found in eleven samples from the Yudachica Member and the Río Salinas Member of the Tiñu Formation. The stratigraphic distribution of the brachiopods is shown in fig. 4 and 5.

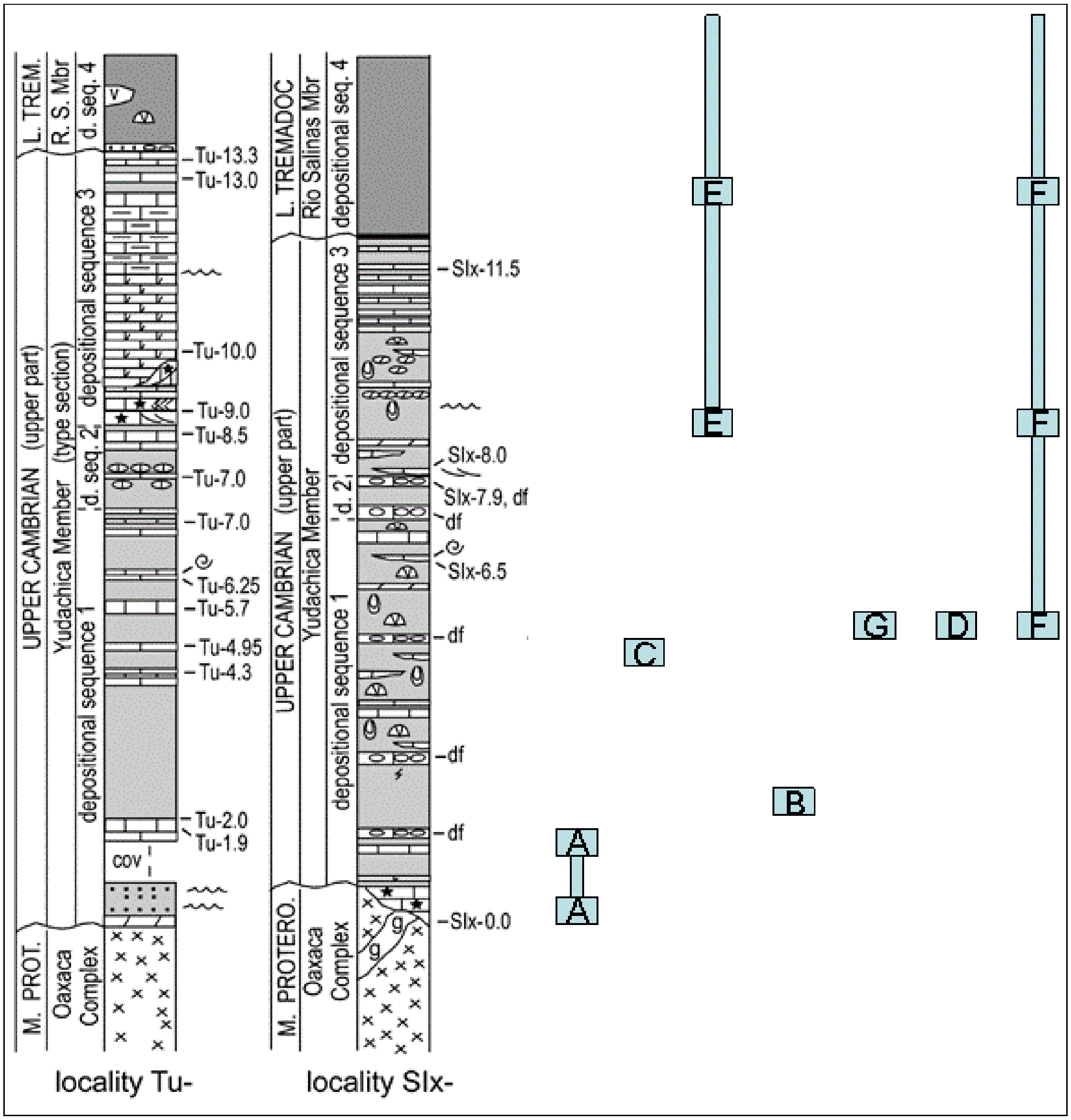

Fig 4. Showing the stratigraphic distribution of Species A, B, C, D, E, F and G.

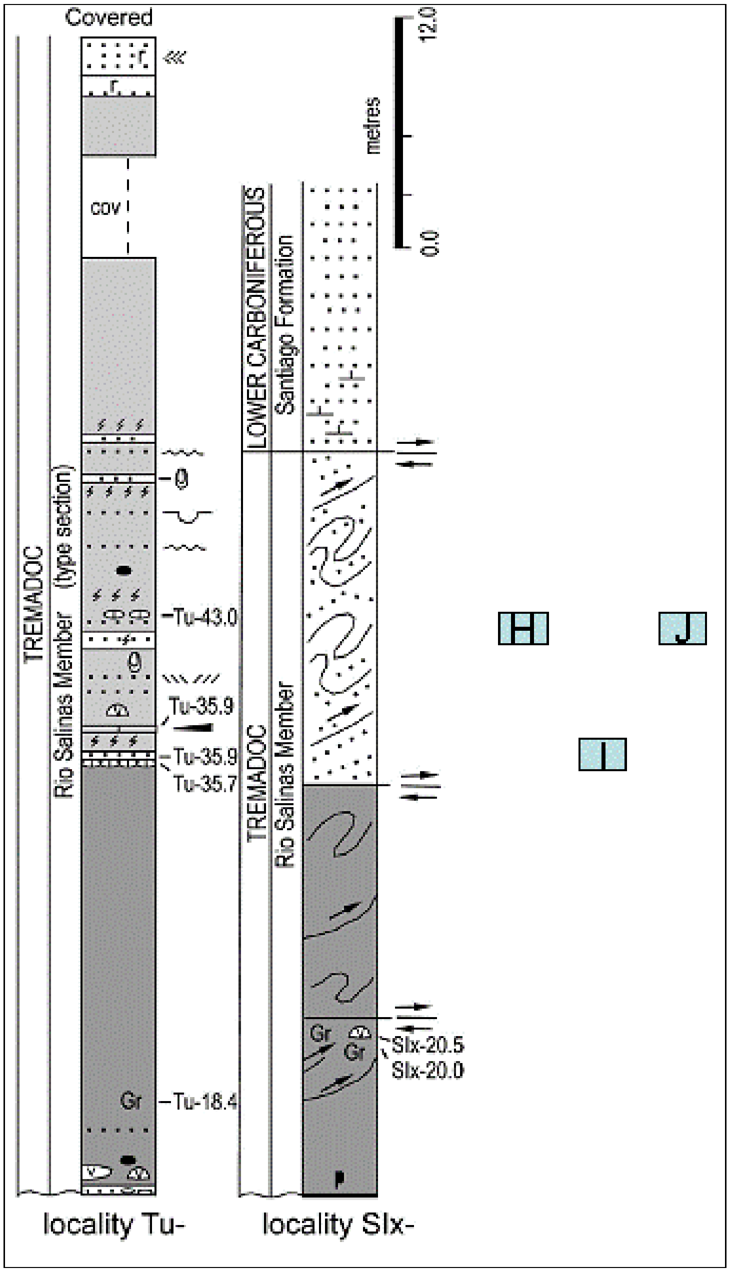

Fig 5. Showing the stratigraphic distribution of Species H, I and J.

Acknowledgements

I want to thank my excellent supervisor Michael Streng for his patience and support during this project. I am truly grateful to my colleague Jan Ove Ebbestad for constantly reminding to finish this project. Thank you Gary Wife for all help with the SEM. Thanks to Ged Malsher and Åsa Frisk for proofreading and to Sandra Pettersson Stolk for being my opponent at my presentation. To all my friends: thanks for making life fun! I thank the Palaeogirls of Uppsala for all the fabulous fikas, and everyone at the Palaeobiology programme and Museum of Evolution for splendid support. Thank you, Mum and Dad, for all support through all my life and for standing by me all the time. And a huge thank you and all my love to Peter for always standing by me, always loving me and always believing in me, even when I did not.

References

Centeno-Garcia, E. and Keppie, J.D, 1999. Latest Paleozoic-early Mesozoic structures in the central Oaxaca Terrane of southern Mexico: deformation near a triple junction. Tectonophysics 301, 231-242

Duméril, A. M. C. 1806. Zoologie analytique ou méthode naturelle de classification des animaux. Allais. Paris. xxiv + 334 p.

Gillis, R.J., Gehrels, G.E., Ruiz, J and Flores de Dios Gonzalez, L.A., 2005. Detrital zircon provenance of Cambrian-Ordovician and Carboniferous strata of the Oaxaca terrane, southern Mexico. Sedimentary Geology 182, 87-100

Gorjansky, V. Iu., and Popov, L. E. 1985. Morfologiia, systematicheskoe polozheniei proiskhozhdenie bezzamkovykh brakhiopods karbonatnoi rakovinoi [Morpholology, systematic position and origin of the inarticulate brachiopods with calcareous shells] Paleontologicheskii Zurnal 1985(3):3-14, 5 fig., 1pl.

Henderson, R. A. and Mackinnon, D. I. 1981. New Cambrian inarticulate Brachiopoda from Australia and the age of the Tasman Formation. Alcheringa 5:289-309, 13 fig.

Holmer, L.E., 1989. Middle Ordovician phosphatic inarticulate brachiopods from Västergötland and Dalarna, Sweden. Fossils and Strata 26: 1-172

Kuhn, Oskar. 1949. Lehrbuch der Paläozoologie. E. Schweizerbart. Stuttgart. v + 326 p., 244 fig.

Kutorga, S. S. 1848. Ueber die Brachiopoden-Familie der Siphonotretaceae. Russisch-Kaiserliche Mineralogische Gesellshaft zu St. Petersbourg, Verhandlungen 1847:250-286, pl. 6-7.

Landing, E., Westrop, S.R. and Keppie J.D., 2007. Terminal Cambrian and lowest Ordovician succession of Mexican West Gondwana: biotas and sequence stratigraphy of the Tiñu Formation .Geol Mag. 144 (5), 1-28

Murphy, J.B., Keppie, J.D., Braid, J.F. and Nance, R.D., 2005. Geochemistry of the Tremadocian Tiñu Formation (Southern Mexico): Provenance in the Underlying ~1 Ga Oaxacan Complex on the Southern Margin of the Rheic Ocean. International Geology Review 45, 887-900

Pantoja-Alor, J. and Robison, R.A., 1967. Paleozoic Sedimentary Rocks in Oaxaca, Mexico. Science 157, 1033-1035

Pantoja-Alor, J., 1970. Rocas sedimentarias paleozoicas de la región centroseprentional de Oaxaca. Sociedad Geológica Mexicana, Libreto-guia de la Excursión México-Oaxaca, pp. 67-84

Robison, R.A. and Pantoja-Alor, J., 1968. Tremadocian Trilobites from the Nochixtlán region, Oaxaca, Mexico. Journal of Paleontology 42 (3), 767-800

Rowell, A. J. 1965. Inarticulata. *In* R. C. Moore, ed., Treatise on Invertebrate Paleontology. Part H, Brachiopoda. The Geological Society of America & The University of Kansas Press. New York and Lawrence. P. 260-296, fig. 158-186.

Rowell, A. J. 1966. Revision of some Cambrian and Ordovician inarticulate brachiopods. The University of Kansas Paleontological Contributions. 7:36p., 33 fig., 4 pl.

Schuchert, Charles. 1893. Classification of the Brachiopoda. American Geologist 11:141-167, pl. 5.

Sobolev, L. P. 1976 Novyi rod bezzamkovykh brakhiopod iz verkhnego kembriia khrebta Dzhagdy (Khabarovskii kray) [A new inarticulate brachiopod genus from the Upper Cambrian of the Dzhagdy Range (Khabarovsk Territory)] Paleontologicheskii Zurnal 1976(2):131-133.

Walcott, C. D. 1884. Palaeontology of the Eureka District, Nevada. United States Geological Survey, Monograph 8:298 p., 24 pl.

Williams, A. and others, 1997. Treatise on Invertebrate Paleontology, part H, Brachiopoda Revised, Vol. 1-3. R. L. Kaesler, editor. Geol. Soc. of America and Univ. of Kansas Press, 919 p

Williams, Alwyn, Carlson, S. J., Brunton, C. H. C., Holmer, L. E. & Popov, L. E. 1996. A supra-ordinal classification of the Brachiopoda. Philosophical Transactions of the Royal Society of London (series B) 351:1171-1193, 6 fig.

Tidigare utgivna publikationer i serien ISSN 1650-6553

Nr 1 **Geomorphological mapping and hazard assessment of alpine areas in Vorarlberg, Austria**, Marcus Gustavsson

Nr 2 **Verification of the Turbulence Index used at SMHI**, Stefan Bergman

Nr 3 **Forecasting the next day's maximum and minimum temperature in Vancouver, Canada by using artificial neural network models**, Magnus Nilsson

Nr 4 **The tectonic history of the Skyttorp-Vattholma fault zone, south-central Sweden**, Anna Victoria Engström

Nr 5 **Investigation on Surface energy fluxes and their relationship to synoptic weather patterns on Storglaciären, northern Sweden**, Yvonne Kramer

Nr 6 **Förekomst och utlakning av bly från Tudors industriområde i Nol**, Anna Bohlin

Nr 7 **Partial Melting in Granulite Gneisses from Hornslandet, SE Central Sweden**, Sofia Carlsson

Nr 8 **Högupplösande processering av seismiska data insamlade nära Gardermoens flygplats**, Marie Larsson

Nr 9 **Sedimentundersökning i Lillsjön och Vikern Gyttorp**, Jan Sävås

Nr 10 **Integrering av MIFO och Grundvattenmodeller**, Marit Brandt

Nr 11 **GIS-baserad förstudie till MKB för behandling av förorenade jordmassor i Stockholms respektive Södermanlands län**, Borka Medjed-Hedlund

Nr 12 **Groundwater Chemistry in the Area East of the Dead Sea, Jordan**, Alice Nassar

Nr 13 **Bly i morän och vatten i delar av Småland, naturligt eller antropogent?**, Karin Luthbom

Nr 14 **Metanflöde mellan väldränerad, subarktisk tundra och atmosfären -betydelsen av markens vattenhalt och kemiska egenskaper**, Gunilla Nordenmark

Nr 15 **Effects of isothermal versus fluctuating temperature regimes on CO_2 efflux from sub-arctic soils**, Pär Eriksson

Nr 16 **En dagvattenmodell för beräkning av avrinning och transport av kväve och fosfor i Flatendiket i södra Stockholm**, Sara-Sofia Hellström

Nr 17 **Långsiktiga effekter av odlingsinriktning på förändringar i markens humusförråd - en fallstudie,** Helena Näslund

Nr 18 **Dynutveckling längs kusten utanför Halmstad, under senare hälften av 1900-talet.** Ingrid Engvall

Nr 19 **Humidity Structures in the Marine Atmospheric Boundary Layer,** Andreas Svensson

Nr 20 **The Influence of Waves on the Heat Exchange over Sea,** Erik Sahlée

Nr 21 **Åska längs Sveriges kuster,** Ulrika Andersson

Nr 22 **En enkel modell för beräkning av tjäldjup,** Johan Hansson

Nr 23 **Modelling the Wind Climate in Mountain Valleys Using the MIUU Mesoscale Model,** Nikolaus Juuso

Nr 24 **Evaluation of a New Lateral Boundary Condition in the MIUU Meso-Scale Model,** Anna Jansson

Nr 25 **Statistisk studie av sambandet mellan geostrofisk vind och temperatur i södra Sverige,** Jonas Höglund

Nr 26 **A comparison of the temperature climate at two urban sites in Uppsala,** Paulina Larsson

Nr 27 **Optiska djupet för atmosfäriska aerosolpartiklar över södra Sverige,** Jonas Lilja

Nr 28 **The wind field in coastal areas,** Niklas Sondell

Nr 29 **A Receiver Function Analysis of the Swedish Crust,** David Mawdsley

Nr 30 **Tjäldjupsberäkningar med temperatursummor,** Malin Knutsson

Nr 31 **Processing and Interpretation of Line 4 Seismic Reflection Data from Siljan Ring Area,** Daniela Justiniano Romero

Nr 32 **Turning Ray Tomography along deep Reflection Seismic Line 4 from the Siljan Ring Area,** Anmar C. Dávila Chacón

Nr 33 **Comparison of two small catchments in the Nopex research area by water balance and modelling approaches,** Ulrike Kummer

Nr 34 **High resolution data processing of EnviroMT data,** Tobias Donner

Nr 35 **Paleoclimatic conditions during late Triassic to early Jurassic, northern North Sea: evidence from clay mineralogy,** Victoria Adestål

Nr 36 **Controlled Source Magnetotellurics - The transition from near-field to far-field** Hermann Walch

Nr 37 **Soil respiration in sub-arctic soils – controlling factors and influence of global change,** Evelina Selander

Nr 38 **Miljöeffekter av Triorganiska tennföreningar från antifoulingfärg – med avseende på sedimentologi, ekotoxikologi och hydrogeologi**, Sara Berglund

Nr 39 **Depth distribution of methanotroph activity at a mountain birch forest-tundra ecotone, northern Sweden,** Erik Melander

Nr 40 **Methyl tert-Butyl Ether Contamination in Groundwater,** Linda Ahlström

Nr 41 **Geokemisk undersökning av vattnet i Västerhavet Med avseende på metallhalter och ^{129}I,** Anette Bergström

Nr 42 **Fracture filling minerals and the extent of associated alteration into adjacent granitic host rock,** Erik Ogenhall

Nr 43 **Bi-Se minerals from the Falun Copper mine,** Helena Karlsson

Nr 44 **Structures and Metamorphism in the Heidal-Glittertindarea, Scandinavian Caledonides,** Erik Malmqvist

Nr 45 **Structure and isotope-age studies in Faddey Bay region of central Taymyr, northern Siberia,** Robert Eriksson

Nr 46 **Stabilitetsindex – en stabil prognosmetod för åska?,** Johan Sohlberg

Nr 47 **Stadsklimateffekter i Uppsala,** Andreas Karelid

Nr 48 **Snow or rain? - A matter of wet-bulb temperature,** Arvid Olsen

Nr 49 **Beräkning av turbulenta flöden enligt inertial dissipationsmetoden med mätdata från en specialkonstruerad lättviktsanemometer samt jämförelse med turbulenta utbytesmetoden,** Charlotta Nilsson

Nr 50 **Inverkan av det interna gränsskiktets höjd på turbulensstrukturen i ytskiktet,** Ulrika Hansson

Nr 51 **Evaluation of the Inertial Dissipation Method over Land,** Björn Carlsson

Nr 52 **Lower Ordovician Acritarchs from Jilin Province, Northeast China,** Sebastian Willman

Nr 53 **Methods for Estimating the Wind Climate Using the MIUU-model,** Magnus Lindholm

Nr 54 **Mineralogical Evolution of Kaolinite Coated Blast Furnace Pellets,** Kristine Zarins

Nr 55 **Crooked line first arrival refraction tomography near the Archean-Proterozoic in Northern Sweden,** Valentina Villoria

Nr 56 **Processing and AVO Analyses of Marine Reflection Seismic Data from Vestfjorden, Norway,** Octavio García Moreno

Nr 57 **Pre-stack migration of seismic data from the IBERSEIS seismic profile to image the upper crust,** Carlos Eduardo Jiménez Valencia

Nr 58 **Spatial and Temporal Distribution of Diagenetic Alterations in the Grés de la Créche Formation (Upper Jurassic, N France),** Stefan Eklund

Nr 59 **Tektoniskt kontrollerade mineraliseringar i Oldenfönstret, Jämtlands län,** Gunnar Rauséus

Nr 60 **Neoproterozoic Radiation of Acritarchs and Environmental Perturbations around the Acraman Impact in Southern Australia,** Mikael Axelsson

Nr 61 **Chlorite weathering kinetics as a function of pH and grain size,** Magdalena Lerczak and Karol Bajer

Nr 62 **H_2S Production and Sulphur Isotope Fractionation in Column Experiments with Sulphate - Reducing Bacteria,** Stephan Wagner

Nr 63 **Magnetotelluric Measurements in the Swedish Caledonides,** Maria Jansdotter Carlsäter

Nr 64 **Identification of Potential Miombo Woodlands by Remote Sensing Analysis,** Ann Thorén

Nr 65 **Modeling Phosphorus Transport and Retention in River Networks,** Jörgen Rosberg

Nr 66 **The Importance of Gravity for Integrated Geophysical Studies of Aquifers,** Johan Jönberger

Nr 67 **Studying the effect of climate change on the design of water supply reservoir,** Gitte Berglöv

Nr 68 **Source identification of nitrate in a Tertiary aquifer, western Spain: a stable-isotope approach,** Anna Kjellin

Nr 69 **Kartläggning av bly vid Hagelgruvan, Gyttorp,** Ida Florberger

Nr 70 **Morphometry and environmental controls of solifluction landforms in the Abisko area, northern Sweden,** Hanna Ridefelt

Nr 71 **Trilobite biostratigraphy of the Tremadoc Bjørkåsholmen Formation on Öland, Sweden,** Åsa Frisk

Nr 72 **Skyddsområden för grundvattentäkter - granskning av hur de upprättats,** Jill Fernqvist

Nr 73 **Ultramafic diatremes in middle Sweden,** Johan Sjöberg

Nr 74 **The effect of tannery waste on soil and groundwater in Erode district, Tamil Nadu, India** *A Minor Field Study*, Janette Jönsson

Nr 75 **Impact of copper- and zinc contamination in groundwater and soil, Coimbatore urban areas, Tamil Nadu, South India** *A Minor Field Study,* Sofia Gröhn

Nr 76 **Klassificering av Low Level Jets och analys av den termiska vinden över Östergarnsholm** , Lisa Frost

Nr 77 **En ny metod för att beräkna impuls- och värmeflöden vid stabila förhållanden**, Anna Belking

Nr 78 **Low-level jets - observationer från Näsudden på Gotland**, Petra Johansson

Nr 79 **Sprite observations over France in relation to their parent thunderstorm system**, Lars Knutsson

Nr 80 **Influence of fog on stratification and turbulent fluxes over the ocean**, Linda Lennartsson

Nr 81 **Statistisk undersökning av prognosmetod för stratus efter snöfall**, Elisabeth Grunditz

Nr 82 **An investigation of the surface fluxes and other parameters in the regional climate model RCA1during ice conditions**, Camilla Tisell

Nr 83 **An investigation of the accuracy and long term trends of ERA-40 over the Baltic Sea**, Gabriella Nilsson

Nr 84 **Sensitivity of conceptual hydrological models to precipitation data errors – a regional study**, Liselotte Tunemar

Nr 85 **Spatial and temporal distribution of diagenetic modifications in Upper Paleocene deep-water marine, turbiditic sandstones of the Faeroe/Shetland basin of the North Sea**, Marcos Axelsson

Nr 86 **Crooked line first arrival refraction tomography in the Skellefte ore field, Northern Sweden**, Enrique Pedraza

Nr 87 **Tektoniken som skulptör - en strukturgeologisk tolkning av Stockholmsområdet och dess skärgård,** Peter Dahlin

Nr 88 **Predicting the fate of fertilisers and pesticides applied to a golf course in central Sweden, using a GIS Tool,** Cecilia Reinestam

Nr 89 **Formation of Potassium Slag in Blast Furnace Pellets**, Elin Eliasson

Nr 90 **- Syns den globala uppvärmningen i den svenska snöstatistiken?**Mattias Larsson

Nr 91 **Acid neutralization reactions in mine tailings from Kristineberg**, Michal Petlicki och Ewa Teklinska

Nr 92 **Ravinbildning i Naris ekologiska reservat, Costa Rica**, Axel Lauridsen Vang

Nr 93 **Temporal variations in surface velocity and elevation of Nordenskiöldbreen, Svalbard**, Ann-Marie Berggren

Nr 94 **Beskrivning av naturgeografin i tre av Uppsala läns naturreservat**, Emelie Nilsson

Nr 95 **Water resources and water management in Mauritius,** Per Berg

Nr 96 **Past and future of Nordenskiöldbreen, Svalbard,** Peter Kuipers Munneke

Nr 97 **Micropaleontology of the Upper Bajocian *Ostrea acuminata* marls of Champfromier (Ain, France) and paleoenvironmental implications,** Petrus Lindh

Nr 98 **Calymenid trilobites (Arthropoda) from the Silurian of Gotland**, Lena Söderkvist

Nr 99 **Development and validation of a new mass-consistent model using terrain-influenced coordinates,** Linus Magnusson

Nr 100 **The Formation of Stratus in Rain,** Wiebke Frey

Nr 101 **Estimation of gusty winds in RCA,** Maria Nordström

Nr 102 **Vädermärken och andra påståenden om vädret - sant eller falskt?,** Erica Thiderström

Nr 103 **A comparison between Sharp Boundary inversion and Reduced Basis OCCAM inversion for a 2-D RMT+CSTMT survey at Skediga, Sweden,** Adriana Berbesi

Nr 104 **Space and time evolution of crustal stress in the South Iceland Seismic Zone using microearthquake focal mechanics,** Mimmi Arvidsson

Nr 105 **Carbon dioxide in the atmosphere: A study of mean levels and air-sea fluxes over the Baltic Sea,** Cristoffer Wittskog

Nr 106 **Polarized Raman Spectroscopy on Minerals,** María Ángeles Benito Saz

Nr 107 **Faunal changes across the Ordovician – Silurian boundary beds, Osmundsberget Quarry, Siljan District, Dalarna,** Cecilia Larsson

Nr 108 **Shrews (Soricidae: Mammalia) from the Pliocene of Hambach, NW Germany,** Sandra Pettersson

Nr 109 **Waveform Tomography in Small Scale Near Surface Investigations,** Joseph Doetsch

Nr 110 **Vegetation Classification and Mapping of Glacial Erosional and Depositional Features** ***Northeastern part of Isla Santa Inés, 53°S and 72°W, Chile,*** Jenny Ampiala

Nr 111 **Recent berm ridge development inside a mesotidal estuary** ***The Guadalquivir River mouth case,*** Ulrika Åberg

Nr 112 **Metodutveckling för extrahering av jod ur fasta material,** Staffan Petré

Nr 113 **Släntstabilitet längs Ångermanälvens dalgång,** Mia Eriksson

Nr 114 **Validation of remote sensing snow cover analysis,** Anna Geidne

Nr 115 **The Silver Mineralogy of the Garpenberg Volcanogenic Sulphide Deposit, Bergslagen, Central Sweden,** Camilla Berggren

Nr 116 **Satellite interferometry (InSAR) as a tool for detection of strain along End-Glacial faults in Sweden,** Anders Högrelius

Nr 117 **Landscape Evolution in the Po-Delta, Italy,** Frida Andersson

Nr 118 **Metamorphism in the Hornslandet Area, South - East Central Sweden,** Karl-Johan Mattsson

Nr 119 **Contaminated Land database -** GIS as a tool for Contaminated Land Investigations**,** Robert Elfving

Nr 120 **Geofysik vid miljöteknisk markundersökning,** Andreas Leander

Nr 121 **Precipitation of Metal Ions in a Reactive Barrier with the Help of Sulphate - Reducing Bacteria,** Andreas Karlhager

Nr 122 **Sensitivity Analysis of the Mesoscale Air Pollution Model TAPM,** David Hirdman

Nr 123 **Effects of Upwelling Events on the Atmosphere,** Susanna Hagelin

Nr 124 **The Accuracy of the Wind Stress over Ocean of the Rossby Centre Atmospheric Model (RCA),** Alexandra Ohlsson

Nr 125 **Statistical Characteristics of Convective Storms in Darwin, Northern Australia,** Andreas Vallgren

Nr 126 **An Extrapolation Technique of Cloud Characteristics Using Tropical Cloud Regimes,** Salomon Eliasson

Nr 127 **Downscaling of Wind Fields Using NCEP-NCAR-Reanalysis Data and the Mesoscale MIUU-Model,** Mattias Larsson

Nr 128 **Utveckling och Utvärdering av en Stokastisk Vädergenerator för Simulering av Korrelerade Temperatur- och Nederbördsserier, för Tillämpningar på den Nordiska Elmarknaden,** Johanna Svensson

Nr 129 **Reprocessing of Reflection Seismic Data from the Skåne Area, Southern Sweden,** Pedro Alfonzo Roque

Nr 130 **Validation of the dynamical core of the Portable University Model of the Atmosphere (PUMA),** Johan Liakka

Nr 131 **Links between ENSO and particulate matter pollution for the city of Christchurch,** Anna Derneryd

Nr 132 **Testing of a new geomorphologic legend in the Vattholma area, Uppland, Sweden,** Niels Nygaard

Nr 133 **Återställandet av en utdikad våtmark, förstudie Skävresjön,** Lena Eriksson, Mattias Karlsson

Nr 134 **A laboratory study on the diffusion rates of stable isotopes of water in unventilated firn,** Vasileios Gkinis

Nr 135 **Reprocessing of Reflection Seismic Data from the Skåne Area, Southern Sweden** Wedissa Abdelrahman

Nr 136 **On the geothermal gradient and heat production in the inner core**
Peter Schmidt

Nr 137 **Coupling of the Weather Research and Forecasting model (WRF) with the Community Multiscale Air Quality model (CMAQ), and analysing the forecasted ozone and nitrogen dioxide concentrations**, Sara Johansson

Nr 138 **Sikt i snöfall - En studie av siktförhållanden under perioder med snöfall**,
Jesper Blomster

Nr 139 **Mineralogy of the hypozonal Svartliden gold deposit, northern Sweden, with emphasis on the composition and paragenetic relations of electrum,** Daniel Eklund

Nr 140 **Kinematic analysis of ductile and brittle/ductile shear zones in Simpevarp and Laxemar subarea,** Emil Lundberg

Nr 141 **Wind Climate Estimates-Validation of Modelled Wind Climate and Normal Year Correction,** Martin Högström

Nr 142 **An Analysis of the Local Weather Around Longyearbyen and an Instrumental Comparison,** Charlotta Petersson

Nr 143 **Flux Attenuation due to Sensor Displacement over Sea,** Erik Nilsson

Nr 144 **Undersökning av luftkvaliteten vid småskalig biobränsleförbränning i två kommuner med modellsystemet VEDAIR,** Stefan Andersson

Nr 145 **CO_2-Variation over the Baltic Sea,** Gustav Åström

Nr 146 **Hur mörkt blir det?** Lena Nilsson

Nr 147 **Master thesis in interpretation of controlled-source radiomagnetotelluric data from Hallandsåsen,** Martin Hjärten

Nr 148 **A Structural and Ore Geological study of the Palaeoproterozoic Stratabound Sala Zn-Pb-Ag deposit, Bergslagen, Sweden,** Nils Jansson

Nr 149 **Numerical exploration of radiative-dynamic interactions in cirrus,** Stina Sjöström

Nr 150 **Modellering av flöden och syrgasförhållanden i Dannemorasjön och dess tillrinningsområde,** Seija Stenius

Nr 151 **Characteristics of convective cloud cluster formation over Thailand through satellite image analysis,** Christian Rosander

Nr 152 **Krossberg som ballast för betong - En studie av standardiserade kvalitetstestmetoder för CE-märkning av betongballast,** Kristina Wikström

Nr 153 **Snöns påverkarn på renarnas vinterbete - en del av projektet isis,** Sofie Fredriksson

Nr 154 **A Sensitivity Analysis of Groundwater Suitability Mapping of the Three-Basin Area in Maputo, Mozambique,** Björn Holgersson

Nr 155 **Using cloud resolving model simulations of tropical deep convection to study turbulence in anvil cirrus,** Lina Broman Beijar

Nr 156 **Validation of the WAM model over the Baltic Sea,** Caroline Berg

Nr 157 **A Simple Method for Calculations of Wake Effects in Wind Farms with Influence of Atmospheric Stability,** Anna Lewinschal

Nr 158 **The Behaviour of the Latent Heat Exchange Coefficient in the Stable Marine Boundary Layer,** Kristina Lindgren

Nr 159 **Utveckling och utvärdering av statistiska metoder för att öka träffsäkerheten hos lokala vindprognoser,** Kristoffer Lager

Nr 160 **A new Arthropod from the Early Cambrian Sirius Passet of North Greenland,** Linda Lagebro